

Walter Heywang
Karl Lubitz
Wolfram Wersing
Editors

SPRINGER SERIES IN MATERIALS SCIENCE 114

Piezoelectricity

Evolution and Future
of a Technology

Springer Series in MATERIALS SCIENCE

Editors: R. Hull R. M. Osgood, Jr. J. Parisi H. Warlimont

The Springer Series in Materials Science covers the complete spectrum of materials physics, including fundamental principles, physical properties, materials theory and design. Recognizing the increasing importance of materials science in future device technologies, the book titles in this series reflect the state-of-the-art in understanding and controlling the structure and properties of all important classes of materials.

- | | |
|--|--|
| 99 Self-Organized Morphology
in Nanostructured Materials
Editors: K. Al-Shamery, S.C. Müller,
and J. Parisi | 107 Organic Semiconductors
in Sensor Applications
Editors: D.A. Bernards, R.M. Ownes,
and G.G. Malliaras |
| 100 Self Healing Materials
An Alternative Approach
to 20 Centuries of Materials Science
Editor: S. van der Zwaag | 108 Evolution of Thin-Film Morphology
Modeling and Simulations
By M. Pelliccione and T.-M. Lu |
| 101 New Organic Nanostructures
for Next Generation Devices
Editors: K. Al-Shamery, H.-G. Rubahn,
and H. Sitter | 109 Reactive Sputter Deposition
Editors: D. Depla and S. Mahieu |
| 102 Photonic Crystal Fibers
Properties and Applications
By F. Poli, A. Cucinotta,
and S. Selleri | 110 The Physics of Organic Superconductors
and Conductors
Editor: A. Lebed |
| 103 Polarons in Advanced Materials
Editor: A.S. Alexandrov | 111 Molecular Catalysts
for Energy Conversion
Editors: T. Okada and M. Kaneko |
| 104 Transparent Conductive Zinc Oxide
Basics and Applications
in Thin Film Solar Cells
Editors: K. Ellmer, A. Klein, and B. Rech | 112 Atomistic and Continuum Modeling
of Nanocrystalline Materials
Deformation Mechanisms
and Scale Transition
By M. Cherkaoui and L. Capolungo |
| 105 Dilute III-V Nitride Semiconductors
and Material Systems
Physics and Technology
Editor: A. Erol | 113 Crystallography and the World
of Symmetry
By S.K. Chatterjee |
| 106 Into The Nano Era
Moore's Law Beyond Planar Silicon CMOS
Editor: H.R. Huff | 114 Piezoelectricity
Evolution and Future of a Technology
Editors: W. Heywang, K. Lubitz,
and W. Wersing |

Volumes 50–98 are listed at the end of the book.

Walter Heywang · Karl Lubitz
Wolfram Wersing

Piezoelectricity

Evolution and Future of a Technology

With 326 Figures



Springer

Prof. Dr. Walter Heywang
Schwabener Weg 9a
85630 Grasbrunn
Germany

Wolfram Wersing
Wagnerfeldweg 10
83346 Bergen
Germany

Dr. Karl Lubitz
Roentgenstr. 20
85521 Ottobrunn
Germany

Series Editors:

Professor Robert Hull
University of Virginia
Dept. of Materials Science and Engineering
Thornton Hall
Charlottesville, VA 22903-2442, USA

Professor Jürgen Parisi
Universität Oldenburg, Fachbereich Physik
Abt. Energie- und Halbleiterforschung
Carl-von-Ossietzky-Strasse 9–11
26129 Oldenburg, Germany

Professor R. M. Osgood, Jr.
Microelectronics Science Laboratory
Department of Electrical Engineering
Columbia University
Seeley W. Mudd Building
New York, NY 10027, USA

Professor Hans Warlimont
Institut für Festkörper-
und Werkstofforschung,
Helmholtzstrasse 20
01069 Dresden, Germany

Springer Series in Materials Science ISSN 0933-033x

ISBN 978-3-540-68680-4 e-ISBN 978-3-540-68683-5

Library of Congress Control Number: 2008930152

© Springer-Verlag Berlin Heidelberg 2008

This work is subject to copyright. All rights are reserved, whether the whole or part of the material is concerned, specifically the rights of translation, reprinting, reuse of illustrations, recitation, broadcasting, reproduction on microfilm or in any other way, and storage in data banks. Duplication of this publication or parts thereof is permitted only under the provisions of the German Copyright Law of September 9, 1965, in its current version, and permission for use must always be obtained from Springer-Verlag. Violations are liable to prosecution under the German Copyright Law.

The use of general descriptive names, registered names, trademarks, etc. in this publication does not imply, even in the absence of a specific statement, that such names are exempt from the relevant protective laws and regulations and therefore free for general use.

Typesetting: Data prepared by SPi using a Springer \TeX macro package

Cover concept: eStudio Calamar Steinen

Cover production: WMX Design GmbH, Heidelberg

SPIN: 1155285 57/856/SPi

Printed on acid-free paper

9 8 7 6 5 4 3 2 1

springer.com

Foreword

Piezoelectricity represents an intriguing property of a dedicated class of materials to directly transform mechanical energy and electrical energy into one another. Despite the fact that the phenomenon of piezoelectricity shows all ingredients to fascinate physicists and engineers alike, it only plays a subordinate role in science education. The reason for this discrepancy is due to the fact that piezoelectricity appears to be a minor physical effect. As a consequence, the revolutionary opportunities and the huge technological development in the recent decades hardly reached the awareness of the public. Nevertheless, just piezoelectric devices comprise an annual turnover of umpteen billion dollars, enabling a system technology that stands for an even larger economical value.

This anthology is intended to contribute to narrowing this gap between high technical and economical importance and low coverage in text book area. In the first part, the fundamentals of piezoelectricity and related phenomena as well as the crystallographic structure of piezoelectric materials are introduced. Prototypical as well as economically relevant classes of piezoelectric materials are described. In the second part, the main part of the book, a broad selection of device applications is presented, which reflects the huge spectrum of functionalities covered by piezoelectric in our world today. The third part deals with the most frequently used characterization methods specifically used for piezoelectric materials and devices. In the fourth part, modeling approaches are covered ranging from empirical thermodynamic theory, via first principles theories of piezoelectric materials, to finite element modeling of devices. The book concludes with a fascinating anticipation of the future evolution of the field.

The volumes address graduate students in material science, solid-state physics, and inorganic chemistry, as well as professional scientists and engineers who are interested in material-based innovations. It also may serve as a reference book for managers who are interested in the economical side of innovations and in potential future markets.

The publishers succeeded in compiling an anthology that creates a bridge between a generic view on piezoelectricity on the one hand and a specific

treatise of many exciting examples on the other. In all parts, the book has been written by the internationally leading experts in the specific areas of piezoelectricity and in material science. In addition to the aforementioned aspects this constitutes a high value on its own.

August 2008

Jülich
Rainer Waser

Foreword

When starting the European Materials Research Society (E-MRS) 25 years ago, the founders wanted to reestablish the famous tradition of the European materials community. The E-MRS conferences in Strasbourg and Warsaw, which attract annually about 3,000 scientists from everywhere in the world, give proof of this successful initiative.

But in our global world it is not sufficient to be a top-player in science, market success must also be included: besides the well-known traditional pillars of Helmholtz, being research and education, innovation has to be included as a third column. Having this in mind, E-MRS has started “evolution and future of a technology” as a new book series, which is to describe exemplary cases of materials-based innovations.

After “Silicon,” “Piezoelectricity” is the second volume of this series. Piezoelectricity itself is an excellent and instructive example: it was discovered as physical phenomenon by the Curie brothers in 1880, but has required new adapted materials and technologies. It was a long and sometimes troublesome way to go for making this initially minor effect a real and sometimes even superior competitor to the electro-dynamic respectively magnetic principal, which for a long time was the only way to transform electrical energy or signals into mechanical ones or vice versa effectively. Novel piezoelectric devices and novel design will open up means which avoid this roundabout in many cases.

The book “Piezoelectricity” is interesting not only for students, scientists, and engineers involved in this field, it is informative also for the entire innovation management in industry and politics. I hope that many books of this kind will follow in the new E-MRS series.

August 2008

Strasbourg
Paul Siffert

Preface

The volume as presented has originated from discussions with the European Materials Research Society. It is to fill a gap concerning the scientific and technical importance of piezoelectricity. We have to thank all who have supported this project, especially the publisher and all our authors for their excellent cooperation. We hope that we were able to meet the mentioned goal in spite of the broad diversity of the whole field.

München
August, 2008

Walter Heywang
Karl Lubitz
Wolfram Wersing

Contents

1 Introduction

<i>L.E. Cross and W. Heywang</i>	1
--	---

Part I Basics and Materials

2 Basic Material Quartz and Related Innovations

<i>A. Ballato</i>	9
-------------------------	---

3 The Role of Ferroelectricity for Piezoelectric Materials

<i>W. Wersing, W. Heywang, H. Beige, and H. Thomann</i>	37
---	----

4 Piezoelectric PZT Ceramics

<i>G. Helke and K. Lubitz</i>	89
-------------------------------------	----

5 Relaxor Ferroelectrics

<i>L.E. Cross</i>	131
-------------------------	-----

6 Piezoelectric Polymers and Their Applications

<i>S. Bauer and F. Bauer</i>	157
------------------------------------	-----

Part II Applications and Innovations

7 Electromechanical Frequency Filters

<i>W. Wersing and K. Lubitz</i>	181
---------------------------------------	-----

8 Ultrasonic Imaging

<i>W. Wersing and R. Lerch</i>	199
--------------------------------------	-----

9 High Effective Lead Perovskite Ceramics and Single Crystals for Ultrasonic Imaging

<i>Y.(J.) Yamashita and Y. Hosono</i>	223
---	-----

10 High-Power Ultrasound Transducers for Therapeutic Applications	
<i>D. Cathignol</i>	245
11 Piezoelectric Motors and Transformers	
<i>K. Uchino</i>	257
12 Piezoelectric Positioning	
<i>S. Arnold, P. Pertsch, and K. Spanner</i>	279
13 Piezoelectric Injection Systems	
<i>R. Mock and K. Lubitz</i>	299
14 Advanced RF Signal Processing with Surface Acoustic Waves on Piezoelectric Single Crystal Substrates	
<i>R. Veith, K. Wagner, and F. Seifert</i>	311
15 Piezoelectric Films for Innovations in the Field of MEMS and Biosensors	
<i>P. Muralt</i>	351
16 Piezoelectric Composites by Solid Freeform Fabrication: A Nature-Inspired Approach	
<i>A. Safari and E.K. Akdoğan</i>	377

Part III Characterisation Methods

17 Microstructural Analysis Based on Microscopy and X-Ray Diffraction	
<i>M.J. Hoffmann, H. Kungl, R. Theissmann, and S. Wagner</i>	403
18 Small Signal Resonance Methods	
<i>W. Wersing</i>	423
19 Large Signal Resonance and Laser Dilatometer Methods	
<i>A. Wolff</i>	445
20 Ferroelastic Characterization of Piezoelectrics	
<i>T. Fett</i>	457

Part IV Multiscale Modelling

21 First-Principles Theories of Piezoelectric Materials	
<i>R.E. Cohen</i>	471
22 Thermodynamic Theory	
<i>G.A. Rossetti, Jr.</i>	493

23 Effective Medium Theories*W. Kreher*517**24 Finite-Element Modelling of Piezoelectric Actuators:
Linear and Nonlinear Analyses***T. Steinkopff*535

Part V The Future

25 Trends in Ferroelectric/Piezoelectric Ceramics*N. Setter*553**Index**571

List of Contributors

E.K. Akdoğan

The Glenn Howatt Electronic
Ceramics Research Laboratory
Department of Materials Science
& Engineering
Rutgers-The State University
of New Jersey, Piscataway
NJ 08854, USA
eka@rci.rutgers.edu

S. Arnold

Physik Instrumente (PI) GmbH
& Co. KG
Auf der Roemerstrasse 1
D-76228 Karlsruhe, Germany
s.arnold@pi.ws

A. Ballato

US Army Communications-
Electronics, Research
Development and Engineering
Center Fort Monmouth
NJ 07703, USA
a.ballato@ieee.org

S. Bauer

Soft Matter Physics
Johannes Kepler University
Altenberger Str. 69
A-4040 Linz, Austria
sbauer@jk.uni-linz.ac.at

F. Bauer

Piezotech S.A. Rue de Colmar 9
F-68220 Héringue
France
francois.bauer@piezotech.fr

H. Beige

Martin-Luther-University
Halle-Wittenberg
Department of Physics
Friedemann-Bach-Platz 6
D-06108 Halle
Germany
horst.beige@physik.uni-halle.de

D. Cathignol

Inserm
Institut national de la santé
et de la recherche médicale
151, cours Albert Thomas
F-69424 LYON Cedex 03
France
cathignol@lyon.inserm.fr

R.E. Cohen

Carnegie Institution
of Washington
Geophysical Laboratory
n5251 Broad Branch RD., N.W.
Washington, DC 20015, USA
cohen@gl.ciw.edu

L.E. Cross

Materials Research Institute
The Pennsylvania State University
187 MRL
University Park, PA 16802
USA
lec3@psu.edu

T. Fett

University of Karlsruhe
Institute for Ceramics
in Mechanical Engineering
Haid-und-Neustrasse 7
D-76131 Karlsruhe
Germany
theo.fett@ikm.uni-karlsruhe.de

G. Helke

CeramTec AG
Innovative Ceramic Engineering
Piezotechnology Lauf, retired
Luitpoldstr. 15
D-91207 Lauf
g.helke@t-online.de

W. Heywang

Siemens AG
Corporate Technology
München, Germany, retired
Schwabener Weg 9a
D-85630 Grasbrunn
Germany
walter.heywang@t-online.de

M.J. Hoffmann

University of Karlsruhe
Institute for Ceramics
in Mechanical Engineering
Haid-und-Neustrasse 7
D-76131 Karlsruhe
Germany
michael.hoffmann@ikm.uka.de

Y. Hosono

Corporate R&D Center
Toshiba Corp.
Kawasaki 212-8582
Japan
yasuharu.hosono@toshiba.co.jp

W. Kreher

Institut für Werkstoffwissenschaft
Technische Universität Dresden
D-01062 Dresden, Germany
wolfgang.kreher@tu-dresden.de

H. Kungl

University of Karlsruhe
Institute for Ceramics
in Mechanical Engineering
Haid-und-Neustrasse 7
D-76131 Karlsruhe, Germany
hans.kungl@ikm.uni-karlsruhe.de

R. Lerch

Department of Sensor Technology
University of Erlangen-Nuremberg
Paul-Gordan-Strasse 3/5
D-91052 Erlangen, Germany
reinhard.lerch@else.eei.
uni-erlangen.de

K. Lubitz

Siemens AG
Corporate Technology
München, Germany, retired
Röntgenstrasse 20
D-85521 München, Germany
karllubitz@t-online.de

R. Mock

Siemens AG
Corporate Technology
Otto-Hahn-Ring 6
D-81730 München, Germany
randolf.mock@siemens.com

P. Muralt

Ceramics Laboratory
EPFL – Swiss Federal
Institute of Technology
(Ecole Polytechnique Fédérale
de Lausanne)
Lausanne 1015
Switzerland
paul.muralt@epfl.ch

P. Pertsch

PI Ceramic GmbH
Lindenstrasse
D-07589 Lederhose
Germany
p.pertsch@piceramic.de

G.A. Rossetti, Jr.

Materials Science and
Engineering Program
Institute of Materials Science
University of Connecticut
Storrs, CT 06269, USA
rossetti@ims.uconn.edu

A. Safari

The Glenn Howatt Electronic
Ceramics Research Laboratory
Department of Materials Science
& Engineering
Rutgers-The State University
of New Jersey, Piscataway
NJ 08854
USA
safari@rci.rutgers.edu

F. Seifert

University of Technology
Vienna Institute of
Sensor- and Actuatorsystems,
retired Gusshausstrasse 27-29
A-1040 Vienna
Austria
franz.seifert@tuwien.ac.at

N. Setter

Ceramics Laboratory
EPFL – Swiss Federal
Institute of Technology
(Ecole Polytechnique Fédérale
de Lausanne)
Lausanne 1015
Switzerland
nava.setter@epfl.ch

K. Spanner

Physik Instrumente (PI) GmbH
& Co. KG
Auf der Roemerstrasse 1
D-76228 Karlsruhe
Germany
k.spanner@pi.ws

T. Steinkopff

Siemens AG
Corporate Technology
Otto-Hahn-Ring 6
D-81730 München
Germany
thorsten.steinkopff@siemens.com

R. Theissmann

University of Duisburg-Essen
Faculty of Engineering
Institute for Nano Structures
and Technology (NST)
Bismarckstr. 81
D-47057 Duisburg
ralf.theissmann@uni-due.de

H. Thomann

Siemens AG
Corporate Technology
München, Germany, retired
Kössener Str. 15
D-81373 München
Germany

K. Uchino

International Center for Actuators
and Transducers
Materials Research Institute
The Pennsylvania State University
University Park
PA 16802, USA
Micromechatronics Inc.
State College, PA 16803
USA
kenjiuchino@psu.edu

R. Veith

EPCOS PTE LTD
166 Kallang Way
Singapore 349249
richard.veith@epcos.com

K. Wagner

EPCOS AG
R&D/Surface Acoustic Wave
Components
Anzinger Strasse 13
D-81671 Munich
Germany
karl.wagner@epcos.com

S. Wagner

University of Karlsruhe
Institute for Ceramics
in Mechanical Engineering
Haid-und-Neustrasse 7
D-76131 Karlsruhe, Germany
susanne.wagner@ikm.uka.de

W. Wersing

Siemens AG
Corporate Technology
München, Germany, retired
Wagnerfeldweg 10
D-83346 Bergen, Germany
wolfram.wersing@t-online.de

A. Wolff

Siemens AG
Corporate Technology
Otto-Hahn-Ring 6
D-81730 München, Germany
andreas.wolff@siemens.com

Y. Yamashita

Toshiba Research Consulting Corp.
Kawasaki 212-8582, Japan
yohachi.yamashita@toshiba.co.jp

Introduction

L.E. Cross and W. Heywang

Barely noticed by the general public, piezoelectricity has become an innovation motor, which worldwide has initiated new markets with turnover of billions of dollars. The piezoelectric market covers a very wide range of technical applications; it is especially strong in the fields of information and communications, industrial automation, medical diagnostics, automation and traffic control, and in the defense industries.

All these innovations are materials based. Thus, on the one hand, the story of piezoelectric innovations cannot be understood as a simple market pull process. On the other hand, a simple science fiction of its inception with statements like “the recently invented class of piezoelectric substances offers many novel possibilities and by exploiting these opportunities an avalanche of novel products will develop changing our lives” does not hold either. Materials-based innovations are usually far more complex. There is mutual stimulation between advances in materials and processing technologies, on the one hand, and technical and economic requirements of new and improved applications on the other, i.e., both market pull and technology push are important inter-correlated factors.

Similarly, the way piezoelectricity entered substantially into the market place was most unusual. Piezoelectricity was first discovered by the Curie brothers in 1880, but not until one century later did we realize the current avalanche of products developing in this market. Interesting questions are what happened during the period of long delay on one hand, and what catalyzed the present avalanche of progress on the other.

From the perspective of solid-state physics, crystalline materials that become electrically polarized when subjected to mechanical stress and conversely change shape when under an applied electric field, namely piezoelectrics, certainly merit study. Technologically, however, the phenomenon only becomes interesting to the broader engineering community when it offers an effect large enough to usefully convert electrical power or signals into mechanical ones or vice-versa. This is the first essential condition, and there are also always a lot of additional needs like small conversion losses, temperature and long

time stability, reproducibility, reliability, cost and other market needs. Out of the family of such requirement for a given device, and the measured material properties, a figure of merit can be formulated. Now we have to compare these figures of merit with the corresponding ones for already existing systems in current applications.

From general experience, it is known that a new novel technology will not succeed in application unless it offers at least a factor of three advantages. Otherwise, in the inertia born tendency for existing solutions to survive, the current approach will be improved by a factor of this order as soon as it is perceived to be endangered.

To effectively enter the market piezoelectrics always had to compete with well-known electromagnetic devices, as for example relays and electromagnetic motors. Only in the case of substantial advantage would they be accepted technically or commercially. Clearly this competition was the major reason for the above-mentioned long delay of the technical break-through to large scale applications.

First time a conceived major improvement in a practical device was achieved through piezoelectricity in 1921 with the development of the quartz crystal stabilized electrical oscillator. In this device, the weak piezoelectricity in quartz is used to excite resonant elastic vibrations where frequency is set by the ultra stable elastic properties of suitable crystal cuts. In 1924, the first crystal stabilized radio transmitter was placed into service, and by late 1930s all high frequency radio transmitters were under crystal control. The astounding success of this initially simple concept is attested by the fact that even now more than 80 years later, the quartz crystal controlled oscillator is still the secondary standard for timing and frequency control.

However, the avalanche of piezo technology starting in the market place was not possible until it was realized that the mixed oxide compound barium titanate (BaTiO_3) was a ferroelectric, and it was demonstrated in 1946 that BaTiO_3 ceramic, which can be easily fabricated and shaped at low price, can be made piezoelectric by an electrical poling process. First commercial piezoelectric devices based on BaTiO_3 ceramics were phonograph pickups and appeared on the market about 1947.

The piezoelectric effect in ferroelectric titanates is much stronger than in quartz because they exhibit different ferroelectric phases with only small energy differences. This can lead to the unusual combination of high dielectric permittivity in a strongly polar lattice in the broad vicinity of the phase boundaries. These conditions are essential for high piezoelectric constants and strong elasto-electric coupling. An advance of great practical importance was the discovery in 1954 of very strong piezoelectric effects in lead zirconate titanate solid solutions. In this material system, a morphotropic phase boundary exists between a tetragonal and rhombohedral ferroelectric phase, which is nearly independent of temperature. Thus, the anomalously high piezoelectric effect near to this boundary is almost constant over a wide temperature

range, important for technical applications. However, one has to pay for the anomalously large piezoelectric effect at this phase boundary with the risk of higher instability of material properties. It was a long and arduous task to control these instabilities by proper adjustment of dopants and grain structure. This problem was eased by the development of two basic material classes adapted to quite different branches of applications: so called soft piezoelectric with as high as possible piezoelectric properties for actuator and ultrasonic applications and so-called hard piezoceramics with as high as possible stability for high power and precise frequency filter applications.

In addition to the material property, considerations on optimum design of device must consider the electrodes through which the field is to be applied. Electrodes must be robust and in very intimate contact with the high permittivity ceramic. Barely any other functional material exists with such a plethora of application-specific shaping requirements: plates, rods, disks, foils, tubes, all designed for either static, dynamic, or resonant applications. There are also composites made from combinations of piezoceramics and plastics, now very widely used in medical ultrasound and in hydrophone systems. Furthermore, to achieve enhanced elongation in actuators at smaller driving voltages, an inexpensive multilayer technology has been developed. In this way, it has become possible to achieve elongations on 0.1 mm in compact monolithic devices, a technology now used for modern fuel valves. These valves react ten times faster than conventional valves and are just revolutionizing motor management in the automotive industry. Thin film technologies are of developing interest for micro electronics and micro electro mechanical (MEMs), for high permittivity dielectric layers, in nonvolatile computer memories, pyroelectric thermal images, and biosensors.

It is very important to recall that beside *polycrystalline piezoelectrics*, ferroelectric piezo-crystals have also been developed. Today we have the stable ferroelectric phase single crystal lithium niobate (LiNbO_3) and lithium tantalate (LiTaO_3). Both are commercially available and widely used for surface acoustic wave devices, which play a major role in signal detection and processing in modern telecommunication systems.

Finally it should be mentioned that there are plastics that can be made ferro- respectively piezoelectric by stress and/or by electrical polarization because of an alignment of asymmetric molecules. They find use as inexpensive foils wherever cheapness or plasticity are relevant., e.g. in cheap microphones or shock gauges. Recent studies following analogous paths to electroceramics have demonstrated effective control of microstructure and properties, stepping stones in bridging to the growing field of biological technologies.

An over-all compilation of existing application of piezoelectricity is given in Table 1.1. The heavy-typed fields indicate where the number of installed piezoelectric samples have exceeded already several billions. Other fields are on the way to follow like the field of automotive applications, where piezoelectric sensors, valves, and injectors are key elements for clean and fuel saving motor

Table 1.1. Piezoelectricity, innovation fields, and important applications

Category	Innovation field	Materials and shaping	Main application
Frequency control and signal processing	Frequency-/time standards	Quartz single crystal plates	Precise frequency control
	Mechanical frequency filters	Ceramic plates of specifically tailored PZT	Inexpensive frequency control and filtering
	Surface acoustic wave (SAW) devices	LiNbO ₃ , LiTaO ₃ , Quartz single crystal substrates	Passive signal processing for wireless communication, identification, sensing, etc.
Sound and ultrasound (US)	Bulk acoustic wave (BAW) devices	Ceramic plates of hard PZT AlN, ZnO thin films	
	Buzzer	Ceramic tapes of soft PZT	Sonic alerts
	Microphones and speakers	Ceramic tapes of soft PZT PZT thin films	Telephone, blood pressure
	Ultrasonic (US) imaging	Diced plates of soft PZT or of PZNT single crystals PZT thin films	Medical diagnostics
	Hydrophonics	Hard PZT of various shapes soft PZT composites	Sources and detectors for sound location
	High power transducers and shock wave generation	Ceramic discs of hard PZT	Machining, US cleaning, lithotripsy
	Atomizer	Ceramic discs of soft PZT	Oil atomizers, humidifiers, aerosols
Actuators and motors	Air ultrasound	Ceramic discs of soft PZT	Distance meter, intrusion alarm
	Printers	Bars, tubes, multilayer ceramics of soft PZT PZT thin films	Needle drives and ink jet
	Motors and transformers	Rings, plates of hard PZT soft PZT multilayer ceramics PZT thin films	Miniaturized, compact motors and transformers
	Bimorph actuators	PZT multilayer ceramics	Pneumatics, micropumps, braille for the blind

	Multilayer actuators	Multilayer stacks of soft PZT	Fine positioning and optics
	Injection systems	Multilayer stacks of soft PZT	Automotive fuel valves
Sensors	Acceleration sensors	Rings, plates of soft PZT	Automotive, automation, medical
	Pressure and shock-wave sensors	LiNbO ₃ substrates	
	Flow sensors	PVDF foils	
	Mass sensitive sensors	Soft PZT discs	
		Quartz discs, Quartz substrates ZnO, AlN thin films	
Ignition	Ignition	Hard PZT cylinders	Gas and fuel ignition
Adaptronics	Adaptive devices	Various shapes of soft PZT, multilayer stacks of soft PZT	Active noise and vibration cancellation, adaptive control, airtail filter control

management. But also in fields where similar figures cannot be expected by nature, piezoelectricity has become a key technology, e.g., wherever ultrasound or mechanical sensing and positioning is concerned.

Furthermore, like every novel technology piezoelectricity has contributed to important scientific achievements or even made them possible. The most famous one is the tunnel microscope and the derived similar instruments for the investigation of atomistic structures. Generally spoken, the effective micro-coupling of mechanical and electric parameters has brought about a better insight into both atomistic as well as phonon-correlated cooperative phenomena.

Summarizing, concerning the multitude of piezoelectric materials and device applications existing already, today we may expect continuous future development and fascinating new novel application areas. Above all we can expect transfer of macrosystems into the micro and nano worlds, the search for lead free and environmentally more friendly highly active piezoelectrics will continue, and last but not least the piezoelectric effect in well textured or even single crystalline Pb(ZrTi)O₃ like systems could surmount the already known strong piezo effects by an order of magnitude enlarging once more the already very broad current field of applications.

Basics and Materials

Basic Material Quartz and Related Innovations

A. Ballato

2.1 General

2.1.1 Commercial and Technological Usages of Quartz

Although material quartz is of scientific interest in its own right, its volume of usage and variety of applications dictate its technological importance. The technological prominence of α -quartz stems largely from the presence of piezoelectricity, combined with extremely low acoustic loss. It was one of the minerals with which the Brothers Curie first established the piezoelectric effect in 1880. In the early 1920s, the quartz resonator was first used for frequency stabilization. Temperature-compensated orientations (the AT and BT shear cuts) were introduced in the 1930s, and assured the technology's success. By the late 1950s, growth of cultured bars became commercially viable, and in the early 1970s, cultured quartz use for electronic applications first exceeded that of the natural variety. The discovery of cuts that addressed compensation of stress and temperature transient effects occurred in the 1970s, and led to the introduction of compound cuts such as the SC, which has both a zero temperature coefficient of frequency, and is simultaneously stress-compensated [1–5]. Between 10^9 and 10^{10} quartz units per year were produced by 2000 at frequencies from below 1 kHz to above 10 GHz. Categories of application include resonators, filters, delay lines, transducers, sensors, signal processors, and actuators. Particularly noteworthy are the bulk- and surface-wave resonators; their uses span the gamut from disposable timepieces to highest precision oscillators for position-location, and picosecond timing applications. Stringent high-shock and high-pressure sensor operations are also enabled. Table 2.1 shows the major applications of quartz crystals. These applications are discussed subsequently in greater detail. For general background and historical developments, see [1, 6–11].

Crystal quartz for timekeeping currently has a global market of over 10^9 USD per year, and that for cellular communications exceeds 50×10^9 USD

Table 2.1. Major applications of quartz crystals

Military and aerospace	Research and metrology	Industrial	Consumer	Automotive
– Communications	– Atomic Clocks	– Communications	– Watches and clocks	– Engine control,
– Navigation/GPS	– Instruments	– Tele-communications	– Cellular and cordless	stereo, clock
– IFF	– Astronomy	– Mobile/cellular/portable	phones, pagers	– Trip computer
– Radar	– and geodesy	radio, telephone, and pager	– Radio and hi-fi equipment	– Navigation/GPS
– Sensors	– Space tracking	– Aviation	– Color TV	
– Guidance systems	– Celestial navigation	– Marine	– Cable TV systems	
– Fuzes		– Navigation	– Home computers	
– Electronic warfare		– Instrumentation	– VCR and video camera	
– Sonobuoys		– Computers	– CB and amateur radio	
		– Digital systems	– Pacemakers	
		– Displays	– Toys and games	
		– Disk drives		
		– Modems		
		– Tagging/identification		
		– Utilities		

per year. Useful rules-of-thumb for the temporal evolution of this technology are the following:

- Upper frequency limit: $f_0 = 10^{+r}$, where f_0 is nominal frequency, $r = 4 + 0.075(Y - 1920)$, and Y is year.
- Frequency accuracy (total fractional absolute frequency variations over all environmental ranges such as temperature, mechanical shock, and aging): $\Delta f/f_0 = 10^{-a}$, where $\Delta f = (f - f_0)$ is frequency shift, and $a = 3.5 + 0.05(Y - 1940)$.
- Aging: $<10^{-8}$ /day for production units, and $<10^{-11}$ /day for high precision units.
- Frequency stability: $\Delta f/f_0 = 10^{-s}$, where $s = 6 + 0.1(Y - X)$, with $X = 1920$ for laboratory versions, $X = 1940$ for commercial versions, and $X = 1960$ for large-scale production models. Observation times are in the range 0.1–10 s. As with Moore’s Law, a saturation of these exponential rates is predicted, but not yet observed.

2.1.2 Phases of the Silica System [12–15]

Silica (SiO_2) is the second most abundant molecule on earth, after H_2O . The phase diagram of the silica system is sketched in Fig. 2.1. This chapter discusses some of the properties and applications of the commercially significant α -quartz phase. Other phases appearing in the diagram are mentioned briefly below.

“Quartz” refers to crystalline α - SiO_2 , arranged in point group symmetry 32 (Hermann-Mauguin)/ D_3 (Schönflies). Figure 2.2 indicates its symmetry elements; z (x_3) is the axis of threefold symmetry. Three equivalent secondary axes x (x_1) are parallel to the twofold axes, and perpendicular to the x_3 axis; three equivalent y (x_2) axes are normal to x_3 and to the respective x_1 axes. The trigonal axis is denoted “optical” (x_3 a screw axis, rotating polarized light), the digonal (x_1) axes are denoted “electrical” and are piezoelectrically active; the x_2 axes are “mechanical” axes. Axial and sign conventions are given in various IEEE Standards and related papers [16–22].

The interlocking nature of the lattice bonds leads to a strong, rigid structure with scratch hardness of 0.667 (with alumina unity), and Moh hardness 7. Si–O bonds occur in pairs with lengths of 0.1598 and 0.1616 nm. Four oxygens coordinate each silicon, with each oxygen slightly off a line joining two neighboring silicons. Bonding is ~ 0.6 covalent and 0.4 ionic, with average bond energies ~ 4.85 eV/bond (~ 0.468 MJ mol $^{-1}$), whereas a single Si–O bond has an energy of 3.82 eV [23]. The unit cell lattice constants are $a_o = 0.4913$ nm, and $c_o = 0.5404$ nm at room temperature [1, 14, 15, 24]. Quartz exhibits enantiomorphism, with chiral (left/right) pairs having space groups $P3_121/D_3^4$ and $P3_221/D_3^6$. Figure 2.3 portrays the external facet arrangement of a completely developed, right-handed specimen.

Upon heating, α - SiO_2 (“low quartz”) undergoes a phase transition at 573.3°C, becoming β - SiO_2 (“high quartz”); in the transition, the silicon atoms

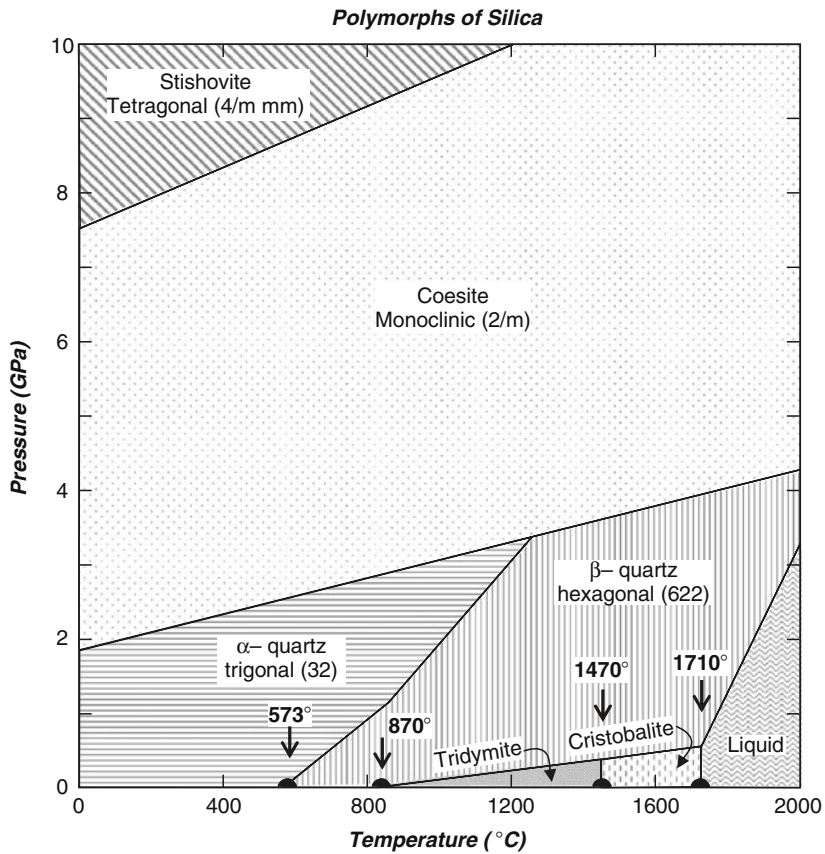


Fig. 2.1. Polymorphs of silica

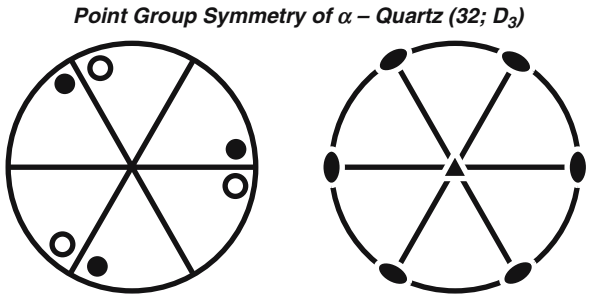


Fig. 2.2. Symmetry elements for α-quartz, point group 32

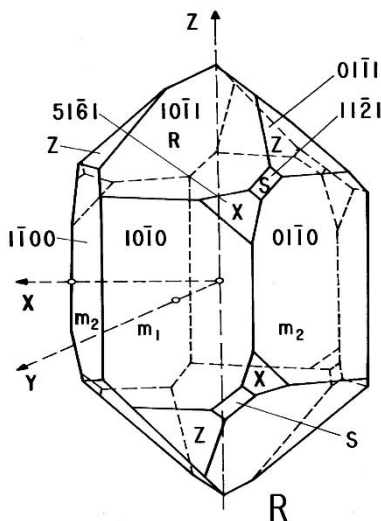


Fig. 2.3. Idealized, right-hand quartz, showing natural facets

move only 0.03 nm, changing the trigonal axis to hexagonal, and the point group symmetry to $622/D_6$. Beta quartz is also enantiomorphic, composed of space groups $P6_222/D_6$ ⁴ and $P6_422/D_6$ ⁵; handedness is preserved in the transition. Enantiomorphism implies the presence of piezoelectricity. Beta quartz is not stable below 573°C. At 600°C, unit cell dimensions are $a_0 = 0.501$ and $c_0 = 0.547$ nm, and density $\rho = 2.533$. α -tridymite (point group uncertain; mmm or $2/m$) is metastable below 870°C, to $\sim 117^\circ\text{C}$; $\rho = 2.28$. β -tridymite ($6/m\ mm$) is stable between 870 and 1,470°C, and metastable down to $\sim 163^\circ\text{C}$; $\rho = 2.24$. α -cristobalite (422) is metastable to below 200°C; $\rho = 2.32$. β -cristobalite ($m3m$) is stable between 1,470 and 1,710°C, and metastable down to 268°C; $\rho = 2.24$. Density units are Mg/m^3 . Coesite is of point symmetry $2/m$; that of stishovite is $4/m\ mm$; both are metastable under ordinary conditions. With the exception of α -cristobalite, the other phases are not piezoelectric. The symmetry diagram for β -quartz is given in Fig. 2.4.

Transitions between different phases of a single polymorph (α - β transformations) involve only bond warping, and not bond breaking; these displacive transformations proceed rapidly. Cooling through the α - β quartz transition invariably results in α -quartz regions having oppositely-directed x_1 axes: “electrical twinning.” Transitions between polymorphs require breaking of bonds; these reconstructive transformations are slow, and subject to kinematic constraints.

Hydrothermal growth of cultured quartz takes place in aqueous NaOH or Na_2CO_3 solutions at temperatures of about 350°C and pressures between 80 and 200 MPa, driven by a temperature gradient from 4 to 10 K. The process

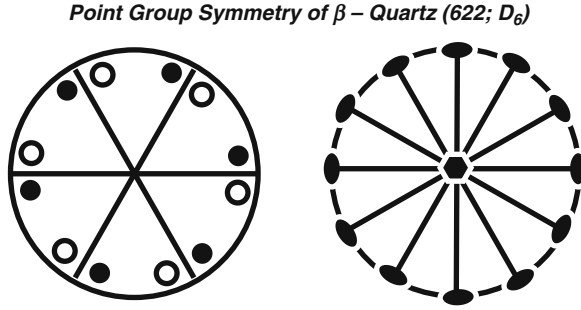


Fig. 2.4. Symmetry elements for β -quartz, point group 622

takes from one to nine months. Processing of quartz crystals includes the steps of cutting, X-ray orienting, lapping, polishing and etching (usually $\text{NH}_4\text{F} \cdot \text{HF}$ or $\text{HF}_{(\text{aq})}$). Growth and etch rates are highly anisotropic, being most rapid along z , with the z rate between 100 and 1,000 times that along x or y axis.

2.2 Phenomenological Coefficients of Quartz

2.2.1 Matter Tensors and Symmetry

Voigt [25] considered field tensors, such as temperature, electric displacement, stress, and strain, and arranged the phenomenological coefficients (matter tensors) relating them according to their ranks. He made the simplification of converting the description of stress and strain from three-dimensional, second-rank tensors to six-dimensional vectors (first-rank tensors). This permits the description of linear elasticity, and related effects, such as piezoelectricity, in simple matrix form. Pertinent here are the intensive field tensors mechanical stress T , electric intensity E , the extensive field tensors mechanical strain S , and electric displacement D . Matter tensors appearing in the constitutive relations are, therefore, elastic stiffness c , and compliance s ; dielectric permittivity ε , and impermeability β ; and piezoelectric constants d , e , g , and h . A graphical portrayal of these relationships was first devised by Heckmann [26], and is now commonly used [1, 27, 28].

The extension of Hooke's Law to piezoelectric coupling between quasi-static mechanical and electrical variables is represented by 9×9 Van Dyke matrices. Four sets are commonly used, depending on the physical structure under consideration, as follows. A prime denotes matrix transpose.

Homogeneous sets:

- (1) $S = s^E T + d' E$ and $D = dT + \varepsilon^T E$
- (2) $T = c^D S - h' D$ and $E = -hS + \beta^S D$

Table 2.2. Van Dyke matrix for the mixed coefficients c^E , e , and ε^S of α -quartz

c_{11}^E	c_{12}^E	c_{13}^E	c_{14}^E	0	0	$-e_{11}$	0	0
c_{12}^E	c_{11}^E	c_{13}^E	$-c_{14}^E$	0	0	e_{11}	0	0
c_{13}^E	c_{13}^E	c_{33}^E	0	0	0	0	0	0
c_{14}^E	$-c_{14}^E$	0	c_{44}^E	0	0	$-e_{14}$	0	0
0	0	0	0	c_{44}^E	c_{14}^E	0	e_{14}	0
0	0	0	0	c_{14}^E	c_{66}^E	0	e_{11}	0
e_{11}	$-e_{11}$	0	e_{14}	0	0	ε_{11}^S	0	0
0	0	0	0	$-e_{14}$	$-e_{11}$	0	ε_{11}^S	0
0	0	0	0	0	0	0	0	ε_{33}^S

Table 2.3. Van Dyke matrix for the homogeneous coefficients s^E , d , and ε^T of α -quartz

s_{11}^E	s_{12}^E	s_{13}^E	s_{14}^E	0	0	d_{11}	0	0
s_{12}^E	s_{11}^E	s_{13}^E	$-s_{14}^E$	0	0	$-d_{11}$	0	0
s_{13}^E	s_{13}^E	s_{33}^E	0	0	0	0	0	0
s_{14}^E	$-s_{14}^E$	0	s_{44}^E	0	0	d_{14}	0	0
0	0	0	0	s_{44}^E	$2s_{14}^E$	0	$-d_{14}$	0
0	0	0	0	$2s_{14}^E$	s_{66}^E	0	$-2d_{11}$	0
d_{11}	$-d_{11}$	0	d_{14}	0	0	ε_{11}^T	0	0
0	0	0	0	$-d_{14}$	$-2d_{11}$	0	ε_{11}^T	0
0	0	0	0	0	0	0	0	ε_{33}^T

Mixed sets:

- (3) $T = c^E S - e' E$ and $D = e S + \varepsilon^S E$
(4) $S = s^D T + g' D$ and $E = -g T + \beta^T D$

Constants d and g are “strain” coefficients; e and h are “stress” coefficients. The $[s^E, d', d, \varepsilon^T]$ and $[c^D, -h', -h, \beta^S]$ matrices are inverses, as are the $[c^E, -e', e, \varepsilon^S]$ and $[s^D, g', -g, \beta^T]$ matrices.

Point-group symmetry dictates the number of components appearing in the constitutive equations coupling the field tensors, and any relations among the components. Tables 2.2–2.5 display the Van Dyke matrices (or “term schemes”) representing point group symmetry 32 and 622. Factors of 2 in the s , d , and g matrices arise from a convention regarding the definition of strain, and, in these tables, $c_{12} = c_{11} - 2c_{66}$ and $s_{12} = s_{11} - s_{66}/2$. The Van Dyke matrices of Tables 2.2 and 2.3, and of Tables 2.4 and 2.5 are inverses of each other.

2.2.2 Numerical Values for α -Quartz

2.2.2.1 Elastic Constants

Alpha-quartz possesses six independent elastic, two piezoelectric, and two dielectric constants. Two principal and competing conventions exist for

Table 2.4. Van Dyke matrix for the mixed coefficients c^E , e , and ε^S of β -quartz

c_{11}^E	c_{12}^E	c_{13}^E	0	0	0	0	0	0
c_{12}^E	c_{11}^E	c_{13}^E	0	0	0	0	0	0
c_{13}^E	c_{13}^E	c_{33}^E	0	0	0	0	0	0
0	0	0	c_{44}^E	0	0	$-e_{14}$	0	0
0	0	0	0	c_{44}^E	0	0	e_{14}	0
0	0	0	0	0	c_{66}^E	0	0	0
0	0	0	e_{14}	0	0	ε_{11}^S	0	0
0	0	0	0	$-e_{14}$	0	0	ε_{11}^S	0
0	0	0	0	0	0	0	0	ε_{33}^S

Table 2.5. Van Dyke matrix for the homogeneous coefficients s^E , d , and ε^T of β -quartz

s_{11}^E	s_{12}^E	s_{13}^E	0	0	0	0	0	0
s_{12}^E	s_{11}^E	s_{13}^E	0	0	0	0	0	0
s_{13}^E	s_{13}^E	s_{33}^E	0	0	0	0	0	0
0	0	0	s_{44}^E	0	0	d_{14}	0	0
0	0	0	0	s_{44}^E	0	0	$-d_{14}$	0
0	0	0	0	0	s_{66}^E	0	0	0
0	0	0	d_{14}	0	0	ε_{11}^T	0	0
0	0	0	0	$-d_{14}$	0	0	ε_{11}^T	0
0	0	0	0	0	0	0	0	ε_{33}^T

determining the signs of certain of the coefficients, and it is necessary to be consistent in following whichever choice is selected [16–22]. Table 2.6 contains experimental values for room-temperature elastic stiffnesses at constant electric field, c^E (isagrig values). Recent results of James [32], indicate that measurement precision is now sufficient to distinguish among the small differences in values occurring between natural and cultured quartz, and between cultured varieties hydrothermally grown either with sodium hydroxide or with sodium carbonate mineralizer. Table 2.7 gives values for the isagrig elastic compliances, s^E corresponding to the entries of Table 2.6.

2.2.2.2 Temperature Coefficients of Elastic Constants

It is found experimentally that a Taylor series expansion to the third order usually suffices to characterize the behavior of the elastic constants of quartz over the often-specified temperature range, -55°C to $+90^\circ\text{C}$. The reference temperature, T_0 , is usually taken to be room temperature. With y standing for any of the elastic stiffnesses or compliances, its value at temperature T is then given by

$$\Delta y/y_0 = T_y^{(1)} \Delta T + T_y^{(2)} (\Delta T)^2 + T_y^{(3)} (\Delta T)^3,$$

Table 2.6. Elastic stiffnesses, c^E

$c_{\lambda\mu}^E$	[25]	[29] ^a	[30]	[31]	[24] ^b	[32]	[33] ^c
c_{11}	85.48	86.75	86.74	86.80	86.80 ± 0.04	86.790	86.7997
c_{13}	14.36	11.3	11.91	11.91	11.91 ± 0.01	12.009	11.9376
c_{14}	-16.83	-17.96	-17.91	-18.04	-18.02 ± 0.07	-18.116	-18.0612
c_{33}	105.6	106.8	107.2	105.75	106.2 ± 0.8	105.79	105.7816
c_{44}	57.13	57.86	57.94	58.20	58.17 ± 0.13	58.212	58.2231
c_{66}	39.11	39.94	39.88	39.88	39.85 ± 0.03	40.000	39.8817
c_{12}	7.25	6.87	(6.98)	(7.04)	7.10 ± 0.09	6.7901	(7.0363)

unit: GPa

^aValues of [34] corrected for piezoelectricity^bAverages gleaned from the literature^cCultured quartz at 23°C**Table 2.7.** Elastic compliances, s^E

$s_{\lambda\mu}^E$	[25]	[29]	[30] ^a	[31]	[24]	[32]	[33]
s_{11}	12.95	12.76	12.77	12.78	12.78	12.779	12.779
s_{13}	-1.53	-1.16	-1.22	-1.24	-1.23	-1.249	-1.238
s_{14}	4.31	4.52	4.50	4.52	-4.52	4.528	-4.525
s_{33}	9.88	9.61	9.60	9.74	9.69	9.736	9.733
s_{44}	20.04	20.09	20.04	19.98	19.99	19.997	19.983
s_{66}	29.28	29.10	29.12	29.17	29.18	29.102	29.172
s_{12}	-1.69	-1.79	-1.79	-1.81	-1.81	-1.772	-1.807

unit: (TPa)⁻¹^aSlightly different values are given in [36] and [37]

where $\Delta y = (y - y_0)$, $\Delta T = (T - T_0)$, and y_0 is the value of y at $T = T_0$. The coefficients $T_y^{(n)}$ are the n th-order temperature coefficients (TCs) of y . Tables 2.8 and 2.9 contain values for the first-order TCs of the stiffnesses and compliances of quartz, respectively. In Tables 2.10 and 2.11 are given the second and third-order stiffness coefficients.

2.2.2.3 Piezoelectric Coefficients and Dielectric Permittivities

Table 2.12 contains values for the piezoelectric coefficients. Table 2.13 lists values for the dielectric permittivities and the impermeabilities, while Table 2.14 gives values for the thermoelastic (thermal expansion) coefficients.

2.2.2.4 Mass Density (ρ)

Natural quartz: $\rho = 2.6487$ at 20°C; 2.649 at 25°C [6]

Cultured quartz: $\rho = 2.6484 \pm 0.0002$ at 25°C [32]; unit: Mg m⁻³

Table 2.8. First-order temperature coefficients of stiffnesses, $T_{C_{\lambda\mu}}^{(1)}$

$\lambda\mu$	[31]	[38]	[39]	[24] ^a	[40]	[32]	[33] ^b
11	-48.5	-44.3	-48.5	-46.4 ± 2.1	-68.2	-43.591	-45.5
13	-383	-492	-550	-476 ± 111	-705	-592.27	-745
14	105	98	101	105 ± 8	84.2	102.59	98.7
33	-153	-188	-160	-172 ± 24	-197	-190.32	-193
44	-158	-172	-177	-170 ± 13	-186	-171.59	-160
66	169	180	178	177 ± 8	158	176.79	166
12	-2,703	-2,930	-3,000 ^c	$-2,901 \pm 183$		-2,640.1	(-2,443)

unit: $10^{-6}/\text{K}$ ^aAverages gleaned from the literature^bCultured quartz at 23°C^c-2,637 for consistency**Table 2.9.** First-order temperature coefficients of compliances, $T_{S_{\lambda\mu}}^{(1)}$

$\lambda\mu$	[31]	[39]	[41]
11	16.5	15.5	8.5
13	-678	-166	-168.8
14	139.5	134	140
33	134.5	140	139.7
44	201	210	211.1
66	-138	-145	-151.9
12	-1,270	-1,370 ^a	-1,296.5

unit: $10^{-6}/\text{K}$ ^a-1,290 for consistency**Table 2.10.** Second-order temperature coefficients of stiffnesses, $T_{C_{\lambda\mu}}^{(2)}$

$\lambda\mu$	[31]	[38]	[39]	[40]	[32]
11	-75	-407	-107	-117	-110.98
13	-2,000	-596	-1,150	-1,022	-1,218.5
14	-270	-13	-48	-54.4	-30.802
33	-187	-1,412	-275	-158	-165.31
44	-212	-225	-216	-272	-254.49
66	-5	201	118	152	156.18
12	-1,500	-7,245	-3,050 ^a		-3,258.7

unit: $10^{-9}/\text{K}^2$ ^a-2,678 for consistency

Table 2.11. Third-order temperature coefficients of stiffnesses, $T_{C_{\lambda\mu}}$ ⁽³⁾

$\lambda\mu$	[31]	[38]	[39]	[40]	[32]
11	−15	−371	−70	−61.9	−99.879
13	600	−5, 559	−750	−43.4	686.06
14	−630	−625	−590	−816	−459.28
33	−410	−243	−250	93.7	−19.089
44	−65	−190	−216	−45.6	−244.95
66	−167	−777	21	−239	102.80
12	1,910	4,195	−1, 260 ^a		−2, 487.8

unit: $10^{-12}/\text{K}^3$
^a−1, 110 for consistency

Table 2.12. Piezoelectric constants

	[38]	[30] ^a	[33] ^b	β -quartz [42]
d_{11}	2.37	2.31		
d_{14}	0.77	0.727		−1.86 ^c
e_{11}	0.175	0.171	0.1719	
e_{14}	−0.0407	−0.0406	−0.0390	−0.067 ^c
g_{11}		0.0578		
g_{14}		0.0182		
h_{11}		4.36		
h_{14}		−1.04		

units: d in pC/N; e in C/m²; g in m²/C; h in N/nC
[30] derived from cgs, rounded
^aSlightly different values are given in [36] and [37]
^bCultured quartz at 23°C; $\rho = 2.64867 \text{ Mg/m}^3$
^cAt 612°C

Table 2.13. Dielectric permittivities, ε , and impermeabilities, β

	[30] ^a	[32]	[33] ^{a,b}
ε_{11}	39.21	39.16	39.136
ε_{33}	41.03	41.04	40.977
β_{11}	25.51	25.54	25.552
β_{33}	24.37	24.37	24.404

units: ε in pF/m; β in m/nF
^a ε^S , β^S
^bCultured quartz at 23°C

Table 2.14. Thermoelastic constants, $\alpha^{(n)}$

	[39]	[43]	[32]	[44] ^a	[33]
$\alpha_{11}^{(1)}$	13.71	13.92	13.77	13.65	13.74
$\alpha_{33}^{(1)}$	7.48	6.79	7.483	7.50	7.48
$\alpha_{11}^{(2)}$	6.50	15.09	13.03	11.02	
$\alpha_{33}^{(2)}$	2.90	8.69	9.405	8.00	
$\alpha_{11}^{(3)}$	-1.90	-7.86	-6.329	-19.32	
$\alpha_{33}^{(3)}$	-1.50	6.88	-5.440	-10.44	

units: $\alpha^{(1)}$ in $10^{-6}/\text{K}$; $\alpha^{(2)}$ in $10^{-9}/\text{K}^2$; $\alpha^{(3)}$ in $10^{-12}/\text{K}^3$

^a-50°C to +150°C

Table 2.15. Acoustic viscosities, η [46]

$\lambda\mu \rightarrow$	11	13	14	33	44	66	(12)
η	1.37	0.72	0.01	0.97	0.36	0.32	0.73

units: η in 10^{-3} Pa s (dekapoise)

- Thermoelastic constants, $\alpha^{(n)}$ See Table 2.14.
- Thermal diffusivity constants, $\alpha_{(\text{td})}$; $\alpha_{(\text{td})11} = 3.3$; $\alpha_{(\text{td})33} = 6.1$; unit: $10^{-6} \text{ m}^2 \text{ s}^{-1}$
- Specific heat capacity, c_p ; $c_p = 740$; unit: J (kg-K)^{-1}
- Thermal conductivity, $k_{(\text{th})}$; $k_{(\text{th})} = \rho c_p \alpha_{(\text{td})}$; $k_{(\text{th})11} = 6.47$; $k_{(\text{th})33} = 12.0$; unit: W (m-K)^{-1}
- Acoustic viscosity, η ; unit: Pa s

Crystal quartz is often treated as lossless [16–21]; but at frequencies above 20 or 30 MHz, loss is usually dominated by internal friction. Lamb and Richter [46] determined acoustic viscosity η as the imaginary part of complex stiffness, $(c^E + j\omega\eta)$. Values for the matrix elements of $\boldsymbol{\eta}$ are given in Table 2.15.

The quotient η/c is the motional time constant, τ_1 , and its value is related to the limiting resonator Q due to intrinsic acoustic attenuation by the relation $Q = (\omega_0\tau_1)^{-1}$.

2.2.2.5 Third-Order Stiffnesses

Quartz resonator frequency shifts caused by environmental disturbances such as acceleration, static forces, and thermal transients have their genesis primarily in elastic nonlinearities. Plane-stress and thermal transient disturbances in quartz resonators may be reduced, or eliminated, by use of certain doubly rotated cuts, notably the BAW SC and SBTC cuts [2–4, 51–54], and the SAW STC cut [55–57]. The necessary measurements of the 14 independent non-Hookean elastic stiffnesses of quartz were first made by Thurston, et al. [58]; see also [59, 60].

2.2.2.6 Recommended Values for α -Quartz

The comprehensive and readable works of Brice [24] and James [32] contain careful and insightful reviews of measurement methods, and of various data sets appearing in the literature. For the linear elastic, piezoelectric, and dielectric constants of quartz, the set obtained by Bechmann [30] using resonator methods is a good choice. The averaged values of Brice [24], and the set derived by James [32] from time-domain method measurements are good alternatives. For the temperature coefficients, the set given in [39], obtained from resonator measurements is a good choice, with the averaged values of Brice [24], and the set derived by James [32] from time-domain method measurements as good alternatives.

2.2.2.7 Beta-Quartz

Beta-quartz possesses five-independent elastic, one piezoelectric, and two dielectric constants, as well as ten independent third-order elastic constants. Table 2.16 lists the measured linear elastic stiffnesses and compliances of β -quartz. Table 2.12 contains the corresponding piezoelectric constants.

2.2.3 Piezoelectric Resonators

By far the greatest technological use of quartz is in piezoelectric resonators and transducers, including sensors. In the 1920s, and into the 1930s, extensional and flexural modes of thin bars and rods were used; in the 1930s into the 1940s, contour modes of plates and discs were used to achieve higher frequencies, since frequency is inversely proportional to the dimension determining the frequency. By the 1950s, driven by the need to reach still higher frequencies, thickness modes of thin plates were used almost exclusively [49, 110–114]. Obtaining requisite thinnesses by ordinary lapping and polishing techniques proved to be an obstacle to achieving fundamental frequencies in excess of about 50 MHz. Frequency requirements in the VHF and UHF ranges, and beyond, led to use of more modern microfabrication technologies that have enabled thickness modes to be realized in thin piezoelectric films.

Table 2.16. Elastic stiffnesses and compliances of β -quartz

$c_{\lambda\mu}^E$	[50]	$s_{\lambda\mu}^E$	[50]
c_{11}	116	s_{11}	9.41
c_{13}	33	s_{13}	−2.6
c_{33}	110	s_{33}	10.6
c_{44}	36	s_{44}	27.7
c_{66}	50	s_{66}	20.02
(c_{12})	16	s_{12}	−0.60

unit: c in GPa; s in (TPa)^{−1}
 T = 600°C

2.2.4 Plate Resonator Cuts

To obtain desirable properties such as temperature compensation, high frequency resonator plates and films must have certain orientations with respect to the crystallographic axes of the crystal. A plate or film, with lateral dimensions large compared with the thickness, can be regarded as a plane, and specified by two orientation angles. Starting from a reference state where the plane normal is along the crystallographic y axis, one rotates the plane about the crystallographic z axis by an angle φ ; the x axis of the plane, originally parallel to the crystallographic x axis, becomes the x' axis. Then, a second rotation is made about the new x' axis by angle θ , creating a compound, or doubly-rotated cut, or orientation. The notation for this operation is $(YXw\ell)\varphi/\theta$ [16]. When angle $\varphi = 0$, the cut is a rotated-Y-cut, with notation: $(YX\ell)\theta$. For further details, see [1, 4, 16, 48, 105, 106].

2.2.5 Equivalent Electrical Circuits

Piezoelectric resonators, filters, transducers, signal processors, sensors, and other acoustic components are invariably incorporated into using systems that are purely electrical. However, because the piezoelectric effect mediates between electrical and mechanical quantities, it is possible to describe the mechanical behavior of these components in purely electrical terms, and thereby to optimize the performance of the overall system. The simplest representation of a resonator is called the Butterworth-Van Dyke (BVD) circuit [107–109], which consists of a capacitor (C_0), representing the driving electrodes, shunted by a “motional” arm consisting of R_1 L_1 C_1 elements in series, representing acoustic loss, mechanical mass, and elastic spring, respectively, of the vibrating crystal. Circuit values depend on the material parameters, mode of motion, and geometry. For transducer applications, provision is made for the presence of mechanical ports in the appropriate equivalent circuits [35, 104–106].

A resonator, represented by the BVD circuit, appears as a capacitive reactance at frequencies below the region of resonance. As resonance is approached, the reactance first becomes zero (“resonance” frequency, f_R), passing into a region of inductive reactance, and reaching a very large value before returning to zero (“antiresonance” frequency, f_A), finally becoming capacitive again at higher frequencies. The region between f_A and f_R (the “pole – zero” spacing) is the normal operating region for an oscillator or filter. This spacing is proportional to the square of the piezoelectric coupling factor (k), discussed in the next paragraph. If this value is small, the oscillator frequency will be confined to a small range, and hence will be very stable; similarly, narrowband filters require small k values, and wideband filters require large k values.

2.2.6 Piezoelectric Coupling Factors

Piezoelectric coupling factors, k , are dimensionless measures of electromechanical energy transduction. In transducers and filters, they determine bandwidth

and insertion loss; in resonators and resonant MEMS devices, they establish pole-zero spacing and adjustment range; in actuators and sensors, they control electromechanical conversion efficiency. In applications, they usually appear as k^2 . For a given type of resonant motion, effective values of elastic, piezoelectric, and dielectric coefficients arise. There are four basic forms expressing coupling, depending upon the constitutive equation set chosen. The generic homogeneous forms are the following:

- $k = |d|/\sqrt{(\varepsilon^T s^E)}$ and $|h|/\sqrt{(\beta^S c^D)}$. The generic mixed forms are:
- $k = |e|/\sqrt{(\varepsilon^S c^E)}$ and $|g|/\sqrt{(\beta^T s^D)}$ [28].

Explicit formulas for some α -quartz resonator plates are the following:

- X-cut (plate normal to x_1 axis): $k_{11} = |e_{11}|/\sqrt{[\varepsilon_{11}^S c_{11}^E + (e_{11})^2]} = 9.23\%$; pure extensional mode, driven by electric field in plate thickness direction.
- Y-cut (plate normal to x_2 axis): $k_{66} = |e_{11}|/\sqrt{[\varepsilon_{11}^S c_{66}^E + (e_{11})^2]} = 13.55\%$; pure shear mode, driven by electric field in plate thickness direction.
- Z-cut (plate normal to x_3 axis): $k_{44} = |e_{14}|/\sqrt{[\varepsilon_{11}^S c_{66}^E]} = 2.69\%$; pure shear mode, motion along direction of driving electric field in $x_2 - x_3$ plane.
- Rotated-Y-cuts (plate normal in $x_2 - x_3$ plane), pure shear mode: $k_{26}' = |e_{26}'|/\sqrt{[\varepsilon_{22}' c']}$; primes denote rotated values. AT cut: $k_{26}' = 8.80\%$ and BT cut: $k_{26}' = 5.62\%$. See Tables 2.17 and 2.18.

Table 2.17. Properties of AT and BT quartz cuts

Quantity	Unit	AT cut	BT cut
Angle	$(YX\ell)\theta$	$\theta = +35.25^\circ$	$\theta = -49.20^\circ$
Tf_R	$10^{-6}/K$	0	0
$\partial Tf_R/\partial\theta$	$10^{-6}/(K, \theta^\circ)$	-5.12	+2.14
$ k $	%	8.80	5.62
v	km/s	3.322	5.073
Z	Mrayl	8.800	13.438
c'_{66}	GPa	29.24	68.16
e'_{26}	C/m ²	-0.0949	-0.0931
ε'_{22}	pF/m	39.82	40.25

Table 2.18. Properties of other rotated-Y-cut quartz cuts

Quantity	Unit	Y cut	Max Tf_R	Min Tf_R	Z cut
Angle	$(YX\ell)\theta$	$\theta = 0^\circ$	$\theta = +4.03^\circ$	$\theta = +69.61^\circ$	$\theta = \pm 90^\circ$
Tf_R	$10^{-6}/K$	+91.11	+94.00	-96.69	-78.53
$\partial Tf_R/\partial\theta$	$10^{-6}/(K, \theta^\circ)$	+0.583	0	0	+1.50
$ k $	%	13.55	13.67	0.562	0
v	km/s	3.916	3.796	4.077	4.677

2.2.7 Properties of Selected α -Quartz Cuts

Table 2.17 contains data pertinent to the shear-mode AT and BT cuts, as these are the preponderant high frequency resonator orientations in current usage. Listed are Tf_R , resonance frequency TC; $\partial Tf_R/\partial\theta$, angle gradient of Tf_R ; $|k|$, effective coupling; v , acoustic velocity; $Z = \rho v$, acoustic impedance; and the related elastic (c_{66}'), piezoelectric (e_{26}'), and dielectric (ε_{22}') values for these cuts. Table 2.18 lists Tf_R , $|k|$, and v data for four other rotated-Y-cuts.

2.3 Innovations: Past and Future

2.3.1 History of Piezoelectric Materials [61]

The phenomenon of piezoelectricity has a very distinguished history. Coulomb conjectured its existence, and later both Haüy and Becquerel conducted unsuccessful experiments. The undoubted discoverers of the phenomenon were the Curie brothers. They knew what they were looking for, had the backgrounds and facilities to bring the search to a successful conclusion, and announced their 1880 discovery as follows [62]:

“Those crystals having one or more axes whose ends are unlike, that is to say hemihedral crystals with oblique faces, have the special physical property of giving rise to two electrical poles of opposite signs at the extremities of these axes when they are subjected to a change in temperature: this is the phenomenon known under the name of pyroelectricity.

“We have found a new method for the development of polar electricity in these same crystals, consisting in subjecting them to variations in pressure along their hemihedral axes.”

The name “piezoelectricity” was given by Hankel; Lippmann predicted the converse effect in 1881, and it was verified by the Curies the same year. Kelvin provided an atomic model in 1893 [63], and theories were advanced by Duhem and Pockels. In 1894, Voigt introduced the term “tensor” describing the phenomenological treatment of this and other effects in crystals. Langevin used Rochelle salt for sonar in the early 1910s, and Born theoretically calculated the piezoconstant of β -ZnS. Cady invented the quartz oscillator in the early 1920s. Tartrates and other water-soluble crystals with large piezoelectric values were investigated in the 1940s and 1950s [64], as were piezoceramics such as barium titanate and similar alloys [65]. Highly piezoelectric refractory oxides such as lithium niobate were introduced in the mid-1960s [66–68], followed by piezopolymers in the late 1960s [69], and isomorphs of quartz in the late 1990s [70–73]. Table 2.19 shows some of the major applications of piezoelectricity. Figure 2.5 portrays the nominal ranges of coupling and quality factor for the various classes of piezoelectrics mentioned. The range for piezopolymers is largely coextensive with that of piezo-semiconductors.

Table 2.19. Major applications of piezoelectricity

Communications and control	Industrial	Health and consumer	Newer applications
<ul style="list-style-type: none">• Cellular radio• Television• Automotive radar	<ul style="list-style-type: none">• Transducers• Sensors• Actuators• Pumps• Motors	<ul style="list-style-type: none">• Transducers• Sensors• Actuators• Pumps• Motors	<ul style="list-style-type: none">• Smart Structures• High Displacement Transducers• Mixed-effect Devices
<ul style="list-style-type: none">– Signal processing– Frequency control and timing	<ul style="list-style-type: none">– Ultrasonic cleaning– Sonar– Nondestructive evaluation (NDE)	<ul style="list-style-type: none">– Noninvasive medical diagnostics– Hyperthermia– Lithotripsy	<ul style="list-style-type: none">– Microelectromechanical (MEMS) devices– Microoptomechnical (MOMS) devices– Biomimetic devices
<ul style="list-style-type: none">– Correlators– Convolvers	<ul style="list-style-type: none">– Liquid level sensors	<ul style="list-style-type: none">– Subcutaneous medication	<ul style="list-style-type: none">– Composite and functionally graded devices
<ul style="list-style-type: none">– Filters– Delay lines	<ul style="list-style-type: none">– Vibration damping– High temperature sensors	<ul style="list-style-type: none">– Wristwatches– Camera focusing/steadying/ranging	<ul style="list-style-type: none">– Rainbow devices– Acousto-phonic-electronic devices
<ul style="list-style-type: none">– Oscillators	<ul style="list-style-type: none">– Material properties determination– Chemical/biological sensors	<ul style="list-style-type: none">– Computer timing/printing/modems– Ignition of gases (“spark pump”)	

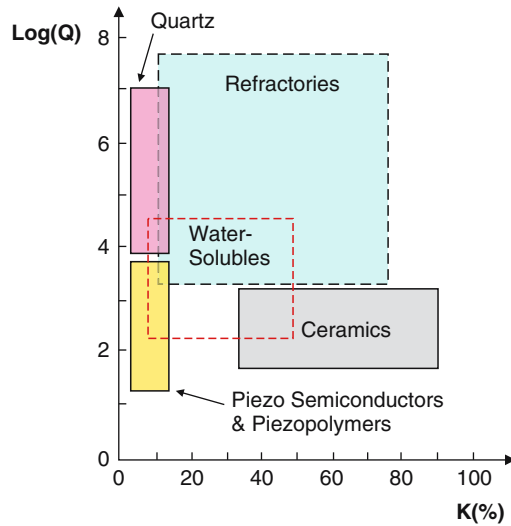


Fig. 2.5. Acoustic quality factor (Q) vs. piezoelectric coupling factor (k) for various types of piezoelectric materials

2.3.2 Current Quartz Uses

Acoustic materials are characterized primarily by elastic linearity, extremely low loss (high quality factor, Q), zero temperature coefficients (ZTCs) of frequency or delay, and particularly by the presence of piezoelectricity. Piezoelectricity provides a clean, efficient transduction mechanism mediating between mechanical motions and electric variables, using planar configurations available with conventional microelectronics fabrication technologies. Even compensation of stress and temperature-transient effects from elastic nonlinearities is possible with quartz, making available high stability bulk acoustic wave (BAW) oscillators. Surface acoustic wave (SAW) substrates provide conveniently accessible time axes for signal processing operations like convolution. The sonic/EM ratio (10^{-5}) affords severe miniaturization in both BAW and SAW devices. For many oscillator applications, it is necessary that the piezocoupling k not be large. This is because the oscillator operating point is confined to the resonator inductive region. Small coupling means a narrow inductive range, and concomitant high oscillator stability.

Acoustic device applications include wireless transceivers for voice, data, multimedia; spread-spectrum (SS) communications for wireless local area networks (WLANs) including WLAN robot, timing, and security applications; components in personal communications system (PCS) handsets, such as duplexers and voltage-controlled oscillators (VCOs); code division multiple access (CDMA) filters and timing; nonvolatile memories, and micro-electromechanical (MEMS)/micro-optomechanical (MOMS) devices. Specific SAW applications are analog signal processing (convolvers, duplexers,

delay lines, and filters) for the mobile telecommunications, multimedia, and industrial-scientific-medical (ISM) bands; wireless passive identification tags, sensors and transponders, and microbalances. BAW applications include resonators in precision clock oscillators; front-end GPS filters for cell phones; thin-film, solidly mounted resonators (SMRs), and stacked crystal filters (SCFs) formed as SMRs, for integration with microwave heterojunction bipolar transistor (HBT) VCOs [5, 8–11].

2.3.3 Usage Considerations

Why quartz? Quartz is the only material known that possesses the following combination of desirable attributes:

- Piezoelectric
- Zero temperature coefficient cuts
- Stress/thermal transient compensated cuts
- Low acoustic loss/high acoustic Q
- Capable of withstanding 35,000–50,000 g shocks
- Very stable
- Capable of integration with micro- and nano-electronic components
- Easy to process; hard but not brittle; under normal conditions, low solubility in everything except fluoride etchants
- Abundant in nature; easy to grow in large quantities, at low cost, and with relatively high purity and perfection. Of the man-made single crystals, quartz, at over 3,000 tonnes per year (2000), is second only to silicon in quantity grown [7].

2.3.4 History of Innovations Related to Quartz that Led to Usages

- 1880
 - Piezoelectric effect discovered: Brothers Pierre & Jacques Curie
- 1900s
 - First hydrothermal growth of quartz in laboratory
- 1910s
 - First application of piezoelectricity, in sonar (Rochelle salt)
 - First quartz crystal oscillator, filter
- 1920s
 - Introduction of quartz resonator; requires “telescope making” technology: rough X-raying; grinding, lapping, polishing
 - Quartz resonator used for frequency stabilization and control
 - First crystal control of radio station
 - BVD equivalent circuit representation
 - Electrical measurements of resonators using oscillators
 - Compound resonator for measuring constants of nonpiezoelectrics
 - First quartz crystal-controlled clock

- 1930s
 - Temperature compensated bulk acoustic wave (BAW) AT/BT cuts developed; requires X-raying to minutes of arc
 - Modal surface motions investigated using lycopodium powder patterns
 - Equivalent circuit incorporating mechanical ports for transducers
- 1940s
 - Hydrothermal growth of quartz [74]; (Czochralski growth of Si and Ge)
 - Electrical measurements using passive transmission networks
 - Electrode system: Al evaporation directly on resonator surfaces
 - Surface finish found to affect quality of resonator
 - First contoured, high-Q, resonator designs
 - Discussion of coupled plate modes [49]
- 1950s
 - Hydrothermal growth of cultured bars commercially viable
 - Solder-sealed metal enclosures
 - Processing ambient: soft vacuum
 - Quartz crystal microbalance (QCM) developed
 - Equivalent circuit in form of acoustic transmission line
 - Temperature-compensated crystal oscillator (TCXO) described
 - Theory of vibrations of anisotropic plates [110]
- 1960s
 - “Energy trapping” theory used to reduce unwanted modes [75–80]
 - Monolithic crystal filter (MCF) developed
 - Solidly mounted resonator (SMR) described
 - Glass enclosures introduced for low aging
 - Electrolytic sweeping reduces effects of ionizing radiation and neutron flux
 - Application of microelectronics technology enabling batch-processing
 - High coupling refractories, such as lithium niobate and tantalate grown
 - Anisotropic plate theory extended [111–113]
- 1970s
 - Cultured quartz use exceeded natural quartz; (Czochralski growth of III-V binaries)
 - Electrical measurements of crystal parameters using bridges
 - Stacked-crystal filters (SCFs) described
 - UV-ozone cleaning to produce atomically clean surfaces and very low aging [81]
 - Chemical polishing reduces subsurface damage; greatly increased shock resistance [82]
 - Temperature and nonlinear effects compensation; requires X-raying to seconds of arc
 - Interdigital transducer (IDT) enables efficient transduction of surface waves [83–87]
 - Surface acoustic wave (SAW) cuts; temperature compensated ST cut
 - Stress-compensated compound cut developed (SC) [2–4]

- Electrical measurements using microcircuit bridges
- Cold-weld metal enclosures
- Processing ambient: cryo-pumps
- Miniature tuning forks (~ 32 kHz) enable quartz wristwatches
- 1980s
 - Stress-compensated BAW compound cut (SBTC) [52–54]
 - Stress-compensated SAW analog of SC cut (STC) [56]
 - Acceleration reduction in SAWs [57]
 - Ceramic flatpack enclosures; high temperature bakeout
 - Microprocessor-compensated crystal oscillator (MCXO) realized
 - Dual mode self-temperature sensing feature applied to MCXO
 - Coupled-mode cuts reduce temperature effects in wristwatch tuning forks
 - Electrode system: high precision air gaps
 - Electrical measurements using network analyzers
 - Processing ambient: ultra-high vacua
- 1990s and 2000s
 - Quartz analogues investigated
 - High stability environmental sensors developed; frequency counting inherently digital
 - Thin film resonator realized (TFR) [88–97]
 - Solidly mounted resonators (SMRs), advanced fabrication makes viable [89–91, 97]
 - Theory of compound-cut, contoured resonators [114]
 - Full-scale finite element method (FEM) models available for 3D simulation of modes

2.3.5 Future Innovations

2.3.5.1 Higher Frequencies

The push to higher frequencies is often dictated by bandwidth considerations. One important criterion by which to measure an acoustic material is its upper frequency limit; the concept is somewhat analogous to the cutoff frequency used for assessing transistors. Maximum usable frequency (f_{\max}) for a piezoelectric resonator is determined jointly by the piezocoupling factor (k) and the acoustic time constant, τ_1 . The relation is $f_{\max} = 2k^2/(\pi^3\tau_1)$, where $\tau_1 = (2\pi f_o Q)^{-1}$, and Q is the measured acoustic quality factor at f_o , the nominal operating frequency [98]. A figure of merit (FOM) often used for piezofilters is (Qk^2) [95]. Thus $f_{\max} = [(4f_o/\pi^2) \cdot (\text{FOM})]$. Put another way, the resonant structure approaches the limit of its usefulness at a normalized frequency (f_{\max}/f_o) approximately 40% of the FOM. A quartz CDMA filter at the 1.9 GHz PCS band typically has an FOM of 120, indicating that

such devices are intrinsically capable of operation at much higher frequencies. Values of f_{\max} from measurements of attenuation and piezocoupling are much higher than frequencies encountered in practice. The discrepancy relates primarily to manufacturing technology, rather than inherent material limitations. For example, AT-cut quartz with $\tau_1 = 11.8$ fs and $k = 8.80\%$, yields $f_{\max} = 42.3$ GHz, a value exceeding present capabilities, but an achievable goal for the future [99].

2.3.5.2 High Coupling Isomorphs of Quartz [70–73]

The search for new materials is fed by practical demands for devices with improved characteristics, e.g., lower loss (higher resonator quality factor (Q), lower filter insertion loss (IL)), higher piezocoupling (k^2) for increased filter bandwidth, better temperature stability, greater miniaturization (higher acoustic velocity), etc. Materials receiving recent attention include the quartz analog langasite and its isomorphs, generically called LGX.

The langasite (LGS, $\text{La}_3\text{Ga}_5\text{SiO}_{14}$) family consists of Czochralski grown, congruently melting, class 32 materials such as langanite (LGN, $\text{La}_3\text{Ga}_{11/2}\text{Nb}_{1/2}\text{O}_{14}$) and langatate (LGT, $\text{La}_3\text{Ga}_{11/2}\text{Ta}_{1/2}\text{O}_{14}$) [70, 71]. Table 2.20 provides pertinent phenomenological data. These materials have acoustic Q s higher than quartz, but have disordered structures, due to the difficulty of satisfying both ionic size and charge compensation constraints. In the future, totally ordered $(\text{Ca}, \text{Sr})_3(\text{Nb}, \text{Ta})\text{Ga}_3\text{Si}_2\text{O}_{14}$ crystals, and similar members, are expected to offer higher elastic stiffnesses, as well as lower dielectric permittivity and higher piezocoupling. Candidate materials include CNGS ($\text{Ca}_3\text{NbGa}_3\text{Si}_2\text{O}_{14}$), CTGS ($\text{Ca}_3\text{TaGa}_3\text{Si}_2\text{O}_{14}$), SNGS ($\text{Sr}_3\text{NbGa}_3\text{Si}_2\text{O}_{14}$), and STGS ($\text{Sr}_3\text{TaGa}_3\text{Si}_2\text{O}_{14}$). Main market possibilities are greater bandwidth (versus quartz), high stability IF filters; high temperature sensors (no twinning); and high Q BAW and SAW resonators [72].

2.3.5.3 Epitaxial Growth of Quartz and Isomorphs

Future miniaturization goals demanded for micro and nano-electromechanical systems (MEMS, NEMS) development [100, 101] will require newer methods of growth and fabrication of thin quartz films and membranes. Recent advances in low-pressure vapor-phase epitaxy [102, 103] open exciting new avenues for future development. Extension of this and other new growth methods applied to quartz and its analogues, such as the totally-ordered LGX family, may yield largely defect-free crystal lattices, and the possibility of achieving greater isotopic constituent purity. Both advances would reduce phonon scattering, realizing significantly higher acoustic Q s, and thereby also further raise the achievable maximum useable frequency [45, 47].

Table 2.20. Material constants of langasite and isomorphs

Quantity	Langasite (LGS)	Langanite (LGN)	Langatate (LGT)
Elastic stiffnesses, $c_{\lambda\mu}^E$ (GPa)			
c_{11}	188.49	192.99	188.52
c_{13}	96.88	102.25	103.36
c_{14}	14.15	14.85	13.51
c_{33}	261.68	264.65	261.80
c_{44}	53.71	49.56	51.10
c_{66}	42.21	41.16	40.32
Temperature coefficients of stiffnesses, $Tc_{\lambda\mu}^E$ ($10^{-6}/K$)			
Tc_{11}	-43.91	-56.34	-78.24
Tc_{13}	-61.95	-31.27	-111.40
Tc_{14}	-309.10	-478.90	-359.60
Tc_{33}	-91.90	-114.70	-102.30
Tc_{44}	-44.05	-14.14	+21.65
Tc_{66}	-22.43	+15.25	-43.63
Piezoelectric stress constants, $e_{m\lambda}$ (C/m ²)			
e_{11}	-0.402	-0.452	-0.456
e_{14}	+0.130	+0.061	+0.094
Dielectric permittivities, $\varepsilon_{ij}/\varepsilon_0$ (dimensionless)			
$\varepsilon_{11}/\varepsilon_0$	19.62	20.09	18.27
$\varepsilon_{33}/\varepsilon_0$	49.41	79.34	78.95
Mass density, ρ (Mg/m ³)			
ρ	5.739	6.029	6.150
Thermoelastic coefficients, α_{ij} ($10^{-6}/K$)			
α_{11}	5.63	6.67	6.09
α_{33}	4.08	5.06	3.83

References

1. W.G. Cady, *Piezoelectricity* (McGraw-Hill, New York, 1946)
2. E.P. EerNisse, in *Proc. 29th Ann. Freq. Control Symp.*, pp. 1-4, US Army Electronics Command, Ft. Monmouth, NJ, May 1975
3. J.A. Kusters, J. Leach, in *Proc. IEEE*, vol. 65, no. 2, pp. 282-284, February (1977)
4. A. Ballato, in *Physical Acoustics: Principles and Methods*, vol. 13, ed. by W.P. Mason, R.N. Thurston. (Academic Press, New York, 1977), Chap. 5, pp. 115-181, ISBN: 0-12-477913-1
5. S. R. Stein, J. R. Vig, in *The Froelich/Kent Encyclopedia of Telecommunications*, Vol. 3, ed. by F.E. Froehlich, A. Kent (Marcel Dekker, New York, 1992) pp. 445-500
6. R.B. Sosman, *The Properties of Silica* (Chemical Catalog Co., New York, 1927)
7. "Quartz crystal," Bulletin 667, Mineral Facts and Problems, US Department of the Interior, Bureau of Mines, 1975

8. A. Ballato, J. R. Vig, in *Encyclopedia of Applied Physics*, Vol. 14, ed. by G. Trigg (VCH Publishers, New York, 1996), pp. 129–145, ISBN: 3-527-28136-3
9. D.J. Jones, S.E. Prasad, J.B. Wallace, *Key Eng. Mater.* **122–124**, 71–144, (1996)
10. *IEEE Trans. Microwave Theory Tech.* **49**(4), part II, 741–847 (April 2001). Special Issue on Microwave Acoustic Wave Devices for Wireless Communications and Sensing. R. Weigel and K. Hashimoto, guest editors
11. R. Weigel, D.P. Morgan, J.M. Owens, A. Ballato, K.M. Lakin, K. Hashimoto, C. C. W. Ruppel, *IEEE Trans. Microwave Theory Tech.* **50**(3), 738–749 (March 2002)
12. C. Frondel, *Dana's System of Mineralogy, Volume II: Silica Minerals*, (Wiley, New York, 1962)
13. B.K. Vainshtein, *Fundamentals of Crystals: Symmetry, and Methods of Structural Crystallography*, 2nd edn. (Springer-Verlag, Berlin, 1994), ISBN 3-540-56558-2
14. B.K. Vainshtein, V.M. Fridkin, V.L. Indenbom, *Modern Crystallography II*, (Springer-Verlag, Berlin, 1982), ISBN 3-540-10517-4
15. C. Klein, C.S. Hurlbut, Jr., *Manual of Crystallography (after J.D. Dana)*, 21st edn. revised, (Wiley, New York, 1999), ISBN: 0-471-31266-5
16. “IRE Standards on piezoelectric crystals, 1949,” *Proc. IRE*, vol. 37, no. 12, pp. 1378–1395, December 1949. (IEEE Standard no. 176)
17. “IRE standards on piezoelectric crystals: determination of the elastic, piezoelectric, and dielectric constants - the electromechanical coupling factor, 1958,” *Proc. IRE*, vol. 46, no. 4, pp. 764–778, April 1958. (IEEE Standard no. 178)
18. “IRE standards on piezoelectric crystals – the piezoelectric vibrator: definitions and methods of measurements, 1957,” *Proc. IRE*, vol. 45, no. 3, pp. 353–358, March 1957
19. “Standard definitions and methods of measurement for piezoelectric vibrators,” IEEE Standard no. 177, (IEEE, New York, May 1966)
20. “IEEE Standard on piezoelectricity,” IEEE Standard 176–1978, IEEE, New York. Reprinted in *IEEE Trans. Sonics Ultrason.*, vol. SU-31, no. 2, Part 2, 55 pp., March 1984
21. “IEEE Standard on piezoelectricity,” IEEE Standard 176–1987, IEEE, New York
22. T.R. Meeker, in *Proc. 33rd Annual Frequency Control Symp.*, pp. 176–180, (Atlantic City, NJ, May-June 1979)
23. L. Pauling, *The Nature of the Chemical Bond*, 3rd edn. (Cornell University Press, Ithaca, 1960). ISBN: 0-8014-0333-2
24. J.C. Brice, *Revs. Mod. Phys.* **57**(1), 105–146 (January 1985)
25. W. Voigt, *Lehrbuch der Kristallphysik* (B.G. Teubner, Leipzig, 1928)
26. G. Heckmann, *Ergeb. exakt. Naturwiss.* **4**, 100–153 (1925)
27. J.F. Nye, *Physical Properties of Crystals* (Oxford University Press, Oxford, 1985). ISBN: 0-19-851165-5
28. A. Ballato, *IEEE Trans. Ultrason., Ferroelec., Freq. Contr.*, **42**(5), 916–926 (September 1995)
29. A.W. Lawson, *Phys. Rev.* **59**, 838–839 (1941)
30. R. Bechmann, *Phys. Rev.* **110**(5), 1060–1061 (June 1, 1958)
31. W.P. Mason, *Bell Syst. Tech. J.* **30**, 366–380 (April 1951)

32. B.J. James, "Determination of the Elastic and Dielectric Properties of Quartz," PhD Dissertation, Royal Holloway and Bedford New College, University of London, Spring 1987, 231 pp. See also B. J. James, "A new measurement of the basic elastic and dielectric constants of quartz," IEEE Intl. Frequency Control Symp. Proc. (42nd Ann.), pp. 146–154, Baltimore, MD, June 1988
33. J. Kushibiki, I. Takanaga, S. Nishiyama, IEEE Trans. Ultrason., Ferroelect., Freq. Contr. **49**(1), 125–135 (January 2002)
34. J.V. Atanasoff, P. J. Hart, Phys. Rev. **59**(1), 85–96 (1941)
35. W.P. Mason, Phys. Rev. **55**, 775–789 (April 1939)
36. R. Bechmann, Proc. Phys. Soc. (London), **B64**, 323–337 (April 1951)
37. R. Bechmann, Archiv der Elektrischen Übertragung **5**, 89–90 (1951). (present name: Archiv für Elektronik und Übertragungstechnik)
38. I. Koga, M. Aruga, Y. Yoshinaka, Phys. Rev. **109**, 1467–1473 (March 1958)
39. R. Bechmann, A. Ballato, T. J. Lukaszek, Proc. IRE **50**(8), 1812–1822 (August 1962); Proc. IRE **50**(12), 2451 (December 1962)
40. P.C.Y. Lee, Y.-K. Yong, J. Appl. Phys. **60**(7), 2327–2342 (1986)
41. J. Zelenka, P.C.Y. Lee, IEEE Trans. Sonics Ultrason. SU-**18**(2), 79–80 (1971)
42. R.K. Cook, P.G. Weissler, Phys. Rev. **80**(4), 712–716 (15 November 1950)
43. A. Ballato, M. Mizan, IEEE Trans. Sonics Ultrason. SU-**31**(1), 11–17 (January 1984)
44. J.A. Kosinski, J.G. Gualtieri, A. Ballato, IEEE Trans. Ultrason., Ferroelec., Freq. Control **39**(4), 502–507 (July 1992)
45. R. Bechmann, in *Landolt-Börnstein, Numerical Data and Functional Relationships in Science and Technology, New Series, Group III: Crystal and Solid State Physics*, ed. by K.-H. Hellwege, A.M. Hellwege (Springer Verlag, Berlin, New York, vol. III/1, pp. 40–123, 1966; and vol. III/2, pp. 40–101, 1969)
46. J. Lamb, J. Richter, Proc. Roy. Soc. (London) **A293**, 479–492 (1966)
47. W.R. Cook, Jr., H. Jaffe, in *Landolt-Börnstein, Numerical Data and Functional Relationships in Science and Technology, New Series, Group III: Crystal and Solid State Physics*, vol. III/11, ed. by K.-H. Hellwege, A.M. Hellwege (Springer Verlag, Berlin, New York, 1979) pp. 287–470
48. B. Parzen, *Design of Crystal and Other Harmonic Oscillators* (Wiley, New York, 1983). ISBN: 0-471-08819-6
49. R.A. Sykes, in *Quartz Crystals for Electrical Circuits: Their Design and Manufacture*, ed. by R.A. Heising (D. Van Nostrand, New York, 1946) Chap. 6, pp. 205–248
50. E.W. Kammer, T.E. Pardue, H.F. Frissel, J. Appl. Phys. **19**(3), 265–270 (March 1948)
51. B.K. Sinha, Ferroelectrics **41**(1), 61–73 (1982)
52. B.K. Sinha, Proc. 35th Annu. Freq. Control Symp. 213–221 (May 1981)
53. M. Valdois, B.K. Sinha, J.-J. Boy, IEEE Trans. Ultrason., Ferroelec., Frequency Contr. **36**(6), 643–651 (November 1989)
54. B.K. Sinha, IEEE Ultrason. Symp. Proc. 557–563 (December 1990)
55. B.K. Sinha, IEEE Trans. Sonics Ultrason. SU-**32**(4), 583–591 (July 1985)
56. B.K. Sinha, IEEE Trans. Ultrason., Ferroelec., Frequency Contr. **34**(1), 64–74 (January 1987)
57. S. Locke, B. K. Sinha, IEEE Trans. Ultrason., Ferroelec., Frequency Contr. UFFC-**34**(4), 478–484 (July 1987)
58. R.N. Thurston, H.J. McSkimin, P. Andreatch, Jr., J. Appl. Phys. **37**(1), 267–275 (January 1966)

59. R. Stern, R.T. Smith, J. Acoust. Soc. Am. **44**, 640–641 (1968)
60. R.F.S. Hearmon, in Landolt-Börnstein, Numerical Data and Functional Relationships in Science and Technology, New Series, Group III: Crystal and Solid State Physics, vol. III/11, ed. by K.-H. Hellwege, A.M. Hellwege (Springer Verlag, Berlin, New York, 1979) pp. 245–286
61. W.P. Mason, J. Acoust. Soc. Am. **70**(6), 1561–1566 (December 1981)
62. P. Curie et, J. Curie, Bull. Soc. Fr. Mineral. Cristallogr. **3**, 90–93 (1880); C. R. Acad. Sci. (Paris) **91**, 294, 383 (March 1880)
63. M. Trainer, Eur. J. Phys. **24**(5), 535–542 (September 2005)
64. R. Bechmann, et al., in *Piezoelectricity* (Her Majesty's Stationery Office, London, 1957), 369 pp
65. D. Berlincourt, J. Acoust. Soc. Am. **70**(6), 1586–1595 (December 1981)
66. T. Yamada, N. Niizeki, H. Toyoda, Japan. J. Appl. Phys. **6**(2), 151–155 (1967)
67. A.W. Warner, M. Onoe, G.A. Coquin, J. Acoust. Soc. Am. **42**(6), 1223–1231 (December 1967)
68. R.T. Smith, F. S. Welsh, J. Appl. Phys. **42**(6), 2219–2230 (May 1971)
69. G.M. Sessler, J. Acoust. Soc. Am. **70**(6), 1596–1608 (December 1981)
70. R.C. Smythe, IEEE Intl. Frequency Control Symp. Proc. 761–765 (May 1998)
71. D.C. Malocha, M.P. da Cunha, E. Adler, R.C. Smythe, S. Frederick, M. Chou, R. Helmbold, Y.S. Zhou, 2000 IEEE/EIA Intl. Freq. Control Symp. Proc., pp. 201–205, Kansas City, MO, June 2000
72. B.H.T. Chai, A.N.P. Bustamante, M. C. Chou, “A new class of ordered langasite structure compounds,” 2000 IEEE/EIA Intl. Freq. Control Symp. Proc., pp. 163–168, Kansas City, MO, June 2000
73. P.W. Krempel, J. Phys. IV France **126**, 95–100 (June 2005)
74. F. Iwasaki, H. Iwasaki, J. Crystal Growth, **237–239**, 820–827 (2002)
75. W. Shockley, D.R. Curran, D.J. Koneval, Proc. 17th Ann. Frequency Control Symp. 88–126 (May 1963)
76. D.R. Curran, D.J. Koneval, Proc. 18th Ann. Freq. Control Symp. 93–119 (May 1964)
77. W.S. Mortley, Wireless World **57**, 399–403 (October 1951)
78. W.S. Mortley, Proc. IEE (London) **104B**, 239–249 (December 1956)
79. R.D. Mindlin, J. Acoust. Soc. Am. **43**(6), 1329–1331 (June 1968)
80. H.F. Tiersten, R.C. Smythe, J. Acoust. Soc. Am. **65**(6), 1455–1460 (June 1979)
81. J.R. Vig, J.W. Le Bus, IEEE Trans. Parts, Hybrids, Packaging **PHP-12**(4), 365–370 (December 1976)
82. J.R. Vig, J.W. LeBus, R.L. Filler, Proc. 31st Ann. Freq. Control Symp. 131–143 (June 1977)
83. R.M. White, F.W. Voltmer, Appl. Phys. Lett. **7**(12), 314–316 (1965)
84. M.B. Schulz, B.J. Matsinger, M.G. Holland, J. Appl. Phys. **41**(7), 2755–2765 (1970)
85. R.M. White, Proc. IEEE **58**(8), 1238–1276 (August 1970)
86. M.G. Holland, L.T. Claiborne, Proc. IEEE **62**(5), 582–611 (May 1974)
87. B.K. Sinha, H.F. Tiersten, Appl. Phys. Lett. **34**(12), 817–819 (15 June 1979)
88. N.F. Foster, J. Acoust. Soc. Am. **70**(6), 1609–1614 (December 1981)
89. W.E. Newell, Proc. IEEE **52**(12), 1603–1607 (December 1964)
90. W.E. Newell, Proc. IEEE **53**(6), 575–581 (June 1965)
91. W.E. Newell, Proc. IEEE **53**(10), 1305–1308 (October 1965)
92. A. Ballato, T. Lukaszek, Proc. IEEE **51**(10), 1495–1496 (October 1973)

93. A. Ballato, H.L. Bertoni, T. Tamir, IEEE Trans. Microwave Theory Tech. **MTT-22**(1), 14–25 (January 1974)
94. K.M. Lakin, G.R. Kline, R.S. Ketcham, J.T. Martin, K.T. McCarron, IEEE Intl. Freq. Control Symp. Proc. 536–543 (May–June 1989)
95. K.M. Lakin, IEEE Intl. Freq. Control Symp. Proc. 201–206 (May 1991)
96. K.M. Lakin, G.R. Kline, K.T. McCarron, IEEE MTT-S Intl. Microwave Symp. Digest **3**, 1517–1520 (June 1993)
97. K.M. Lakin, IEEE Microwave Magazine **4**(4), 61–67 (December 2003)
98. A. Ballato, J.G. Gualtieri, IEEE Trans. Ultrason., Ferroelect., Freq. Contr. **41**(6), 834–844 (November 1994)
99. H. Iwata, IEICE Electronics Express **1**(12), 346–351 (September 2004)
100. K.L. Ekinci, M.L. Roukes, Rev. Sci. Instrum. **76** art. 061101, 12pp. (2005)
101. MEMS: A Practical Guide to Design, Analysis, and Applications, ed. by J.G. Korvink, O. Paul (Springer-Verlag, Heidelberg 2006), ISBN: 3-540-21117-9
102. N. Takahashi, T. Nakumura, S. Nonaka, H. Yagi, Y. Sinriki, K. Tamanuki, Electrochemical and Solid State Lett. **6**(5), C77–C78 (2003)
103. N. Takahashi, T. Nakumura, Electrochemical and Solid State Lett. **6**(11), H25–H26 (2003)
104. A. Ballato, IEEE Trans. Ultrason., Ferroelect., Freq. Contr., **48**(5), 1189–1240 (September 2001)
105. R. A. Heising (ed.), *Quartz Crystals for Electrical Circuits: Their Design and Manufacture* (D. Van Nostrand, New York, 1946)
106. W.P. Mason, *Piezoelectric Crystals and their Application to Ultrasonics* (Van Nostrand, New York, 1950)
107. A. Ballato, Proc. IEEE **58**(1), 149–151 (January 1970)
108. B.A. Auld, *Acoustic Fields and Waves in Solids*, Vol. I and II, (Robert E. Krieger Publishing, Malabar, FL, 1990). ISBNs: 0-89874-783-X; 0-89874-782-1
109. W.P. Mason, Proc. IEEE **57**(10), 1723–1734 (October 1969)
110. R.D. Mindlin, J. Appl. Phys., **23**(1), 83–88 (January 1952)
111. R.D. Mindlin, D.C. Gazis, Proc. Fourth U. S. Natl. Congr. Appl. Math. 305–310 (1962)
112. R.D. Mindlin, P.C.Y. Lee, Intl. J. Solids and Struct. **2**(1), 125–139 (January 1966)
113. R.D. Mindlin, W.J. Spencer, J. Acoust. Soc. Am. **42**(6), 1268–1277 (December 1967)
114. B.K. Sinha, IEEE Trans. Ultrason., Ferroelec., Frequency Contr. **48**(5), 1162–1180 (September 2001)

The Role of Ferroelectricity for Piezoelectric Materials

W. Wersing, W. Heywang, H. Beige, and H. Thomann

Most of the technological applications of piezoelectricity used nowadays are based on ferroelectric materials. This is due to the following reasons:

1. Because of the high piezoelectric effect that can be found in these materials, a high and efficient electromechanical transformation of energy and signals can be achieved.
2. In general, the remnant electrical polarization that occurs in these materials can be oriented into a desired direction by applying an external electrical field: this means by poling, if needed, at elevated temperature. Therefore it becomes possible to imprint a unipolar direction of macroscopic preference or anisotropy to a device even after processing it. Obviously, this unipolarity is mandatory for every piezoelectric action.
3. Therefore, materials that are macroscopically isotropic by nature after the production process can be also used. This concerns, e.g., ceramics, plastics, or composites, which can be processed using well-known methods to adapt and shape the material according to the requirements of the final use.
4. For piezoelectric applications, the group of ceramics based on the so-called perovskite structure is especially important. These materials are already being used over a broad field of technological applications such as in capacitors and PTC resistors¹. Therefore, experience in the mass production, reliability, etc. of these materials is already available.
5. Therefore, also from the point of view of production cost, ferroelectric materials offer good advantages.

Consequently, it makes sense to offer here a short introduction into this class of materials.

¹ PTC: Giant Positive Temperature Coefficient of resistivity within the ferroelectric Curie-Weiss region.

3.1 Fundamental Principles of Ferroelectricity

The name ferroelectricity was chosen because of some principal analogies to ferromagnetism²:

- Below a certain phase transition temperature, the so-called Curie temperature T_C , a spontaneous polarization P_s occurs in ferroelectric materials similar to the spontaneous magnetization in ferromagnetic materials.
- Above T_C , the temperature dependence of the dielectric permittivity ε follows a Curie–Weiss law (Eq. 3.1), just as the magnetic permeability of ferromagnetic materials does.

$$\frac{\varepsilon}{\varepsilon_0} = \frac{C}{T - T_0}. \quad (3.1)^3$$

- To minimize depolarizing fields, different regions of the crystal are polarized in different directions of a possible P_s , each volume of uniform polarization being called a *ferroelectric domain* similar to ferromagnetic domains.
- In the ferroelectric state (below T_C), the dielectric behavior, i.e., the dependence of dielectric displacement \mathbf{D} on electric field strength \mathbf{E} , is highly nonlinear and shows a characteristic hysteresis loop similar to the dependence of the induction \mathbf{B} on magnetic field strength \mathbf{H} in ferromagnetic materials.

However, besides these analogies decisive differences also exist, differences that are important especially in the context of piezoelectricity. Basically, these differences are due to the fact that there does not exist an electrical counterpart to the atomic spin. Thus every electrical dipole requires particle displacements, which influence the structure of the lattice. Consequently, permanent polarization itself causes lattice distortions, changing the lattice symmetry remarkably. As long as we consider the polarization being the major reason for these distortions, we may speak about ferroelectric phases or phase systems.

In Sect. 3.1 we try to understand such systems and to correlate them with the atomic lattice structure conceptually. Using the model of a hypothetical single-domain crystal, the thermodynamic correlations with piezoelectricity will be deduced.

In Sect. 3.2 we will deal with the fact that single crystals, and even more polycrystalline ceramics, cannot be described by single-domain models. Apparent charges have to be compensated either by domain splitting or by ions;

² In spite of ethymologically meaningless, the name “ferroelectricity” has been accepted generally. Ferroelectric properties had been found in Seignette-salt before. Therefore in past times the name Seignette-electricity had been used, particularly in the Russian literature.

³ ε_0 : vacuum permittivity, T_0 : Curie-Weiss temperature; $T_0 < T_C$ in case of a first order phase transition (see also Eq. 3.16), $T_0 = T_C$ in case of a second order (continuous) phase transition.

stresses have to be minimized. The properties of such samples are called *intrinsic*, as long as the domain configuration is not changed by the measuring signal. A conceptual overview will try to explain the interrelation between these intrinsic properties on one hand, and their dependence on composition as well as on preparation and poling procedure on the other.

Section 3.3 finally deals with the same properties in the case that a reorientation of the domains becomes possible under the influence of the measuring signals themselves. We call these properties *extrinsic*.

It should be emphasized again that the aim of this chapter is only to provide a conceptual understanding of possibilities and limitations of piezoelectric material engineering. It should be sufficient for the understanding of the different applications. A more profound description of the state of the art of materials and device design is given in Chap. 12.

3.1.1 Basic Properties of Ferroelectrics

In contrast to quartz, in which we find a preformed asymmetry due to the atomic structure of the lattice, in ferroelectric materials this asymmetry does not exist above the Curie temperature as in ferromagnetic materials. But at the Curie temperature it develops because of the so-called internal (or local) electrical field \mathbf{E}_i , which corresponds to the sum of the applied external field \mathbf{E} and the feedback of the internal dipoles by means of the existing polarization \mathbf{P} :

$$\vec{E}_i = \vec{E} + \frac{\beta}{\varepsilon_0} \vec{P} \quad (3.2)$$

with β being the Lorentz factor.

So far, we have dealt with an exact analogy with magnetism. However, this analogy does not include the nature of the dipoles themselves. In the ferromagnetic case, these dipoles are mainly based on the spin of the single particles. In the electrical case, dipoles cannot be formed without the cooperation of several particles that virtually occupy the lattice. This can be the cloud of electrons surrounding an atomic nucleus or molecule-like structures exhibiting a bond angle, or ions with a displacement relative to the surrounding lattice. Sometimes, such local dipoles already exist above the Curie temperature and are ordered below it under the influence of the internal field; some times they do not form except under the influence of the internal field itself. Depending on the prevalence of the first or the second mechanism, two basically different types of ferroelectric materials are distinguished nowadays:

1. Ferroelectric materials exhibiting dipoles or dipole-like structures that are randomly oriented above the Curie temperature and that will be ordered below, where they give rise to a spontaneous polarization (order-disorder type); and

2. Ferroelectric materials where the lattice cells are not polarized except under the influence of the internal field below the Curie temperature. In this case, the spontaneous polarization is based on the relative displacement of sublattices formed by ions and their electron clouds (displacive type).

But we should state already here that in every ferroelectric material both these mechanisms coexist, even though to different extents. On one hand, dipoles that are preformed in the paraelectric state grow in size by the influence of the internal field below the Curie temperature; on the other, purely ionic bonded crystals cannot undergo a transition to a ferroelectric phase, but become antiferroelectric owing to reasons of electrostatics. Angular bonds, which are mandatory for the development of ferroelectricity, cannot be formed except under the influence of covalent contributions.

From the explanation of ferromagnetism, the thermodynamic statistics of an order–disorder transition is well known. It can be understood as a consequence of dipole orientation within the internal field.

The case of a displacive ferroelectric transition is more complex, especially since there does not exist a well-defined borderline between dipoles and the surrounding lattice. Therefore at this stage a simple introduction to features of such transitions could be helpful. A more thorough explanation and quantitative results cannot be given here, extended outlines are presented in Chap. 12.

The most representative materials among the displacive ferroelectrics are the perovskites, of which a prototype is BaTiO_3 (BT), the lattice structure of which is depicted in Fig. 3.1. The core of the essentially cubic lattice cell is formed by an oxygen octahedron with a 4-valent titanium ion in the center. Neutrality and steric stability of the lattice is ensured by the 2-valent barium ions at the corners of the unit cell. The essential part of the cell that concerns the ferroelectric and piezoelectric properties is represented by the TiO_6 octahedron. This can be expected not only because of the high permittivity

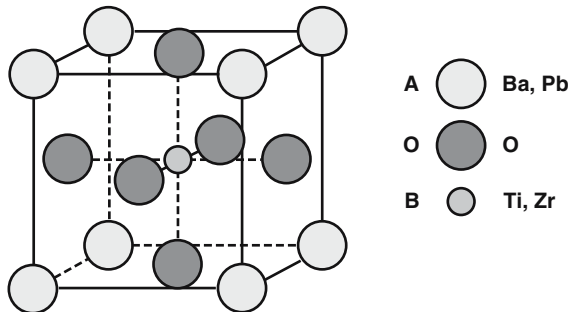


Fig. 3.1. The perovskite structure ABO_3 . BaTiO_3 is the prototype ferroelectric that crystallizes in this structure. Other important examples are PbTiO_3 and $\text{Pb}(\text{Zr}_x\text{Ti}_{1-x})\text{O}_3$

found in all titanium oxides themselves, but also because of the fact that the temperature-independent quotient

$$\frac{TC\varepsilon}{\varepsilon/\varepsilon_0} = \frac{1}{\varepsilon} \frac{d\varepsilon}{dT} \cdot \frac{\varepsilon_0}{\varepsilon} = -\frac{1}{C} \cong -10^{-5} \text{K}^{-1} \quad (3.3)$$

as represented by the Curie–Weiss law of BT can be found in equal magnitude within all TiO_2 compounds independent of their specific lattice structure [1].

Additionally, the reason for the development of a ferroelectric phase instead of an antiferroelectric one below the Curie temperature can be found within the TiO_6 octahedra themselves and their interaction. For, the electrostatic preference of the mutual saturation of the apparent charges at the ends of dipole chains is overcompensated by contributions of the homopolar parts of the Ti–O bonds. It has been shown by X-ray fine structure investigations of BT [2] that already above the Curie temperature a closer binding between the Ti ion and three of its closest oxygen neighbors exists, causing a minor deviation from the central position and the formation of a tetrahedron-like TiO_3 configuration. But owing to the minor energy contribution of this deviation the Ti ion changes the possible partners, continuously oscillating from one position to the other. The average position is found in the center of the unit cell.

The preference for a smaller atomic distance between the Ti ion and its oxygen partners is due to the homopolar part of the Ti–O bond. Furthermore, this homopolar contribution involves also the tendency of oxygen towards angled valencies. This tendency is well known, e.g., from the water molecule, and plays an important role in ferroelectricity. For, it favors the parallel orientation of the polarization in neighboring lattice cells as illustrated in Fig. 3.2. In other words, it causes the transition to ferroelectricity instead of antiferroelectricity below the Curie temperature.

The transition from the paraelectric to the ferroelectric state, which we have concentrated on up to now, is not the only ferroelectric phase transition occurring in BT. This can be seen, e.g., by the results shown in Fig. 3.3. Here Fig. 3.3a shows the temperature dependence of permittivity of

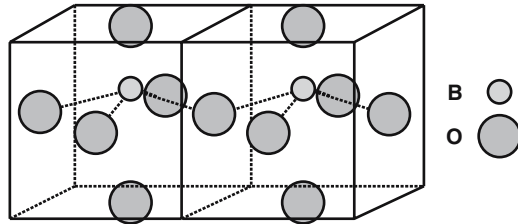


Fig. 3.2. The homopolar contribution of the Ti–O bond involving the tendency of oxygen towards angled valencies, which favors the parallel orientation of the polarization in neighbouring lattice cells

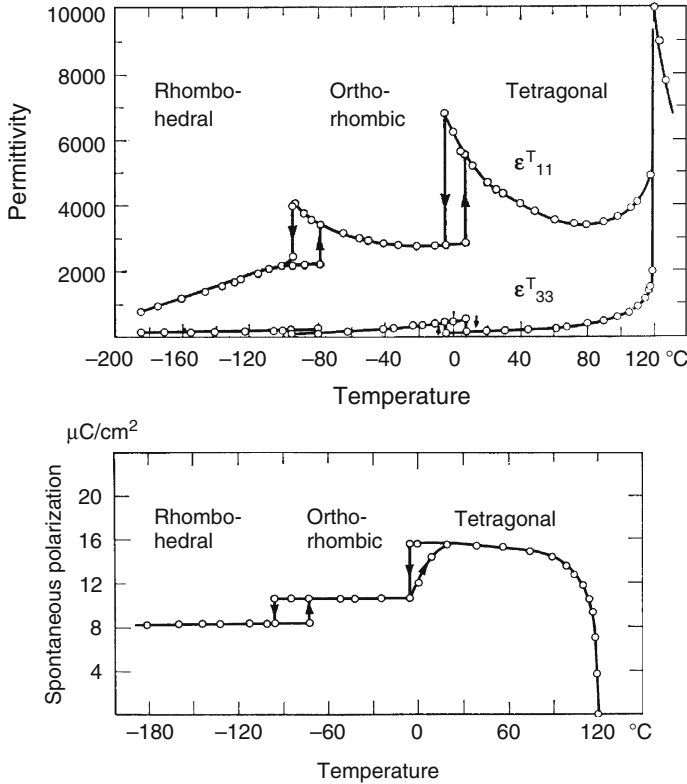


Fig. 3.3. (a) Dielectric constants of BaTiO_3 vs. temperature. The values of ϵ_{11}^T and ϵ_{33}^T in the tetragonal phase refer to single-domain crystals (according to Merz [3]). (b) Spontaneous polarization of BaTiO_3 vs. temperature, measured along the pseudo-cubic (001) edge, i.e., parallel to the 3-axis in the tetragonal phase (according to Merz [3]). In the orthorhombic phase or in the rhombohedral phase, the magnitude of P_s is obtained by multiplying the value in Fig. 3.3b with $\sqrt{2}$ or $\sqrt{3}$, respectively. The onset of P_s at T_C appears to be rather continuous. Although this was found to be due to crystal imperfections, it shows that the transition is only weakly first order

(100)-oriented BT single crystals as measured by Merz [3]. It reveals two more phase transitions below the Curie temperature, which occur when lowering the temperature by about 100 and 200°C, respectively, below T_C . Figure 3.3b explains more explicitly what is going on. Below the Curie temperature, first a spontaneous polarization develops in the (100) direction; at about 10°C this polarization turns into a (110) direction. At -70°C it turns again and finds its final orientation in a (111) direction. Furthermore, at every transition the absolute value of polarization increases remarkably. Corresponding to the polarization the lattice distortion changes from the undistorted cubic phase above the Curie temperature to a tetragonal phase below, then to an orthorhombic one and finally to a rhombohedral one.

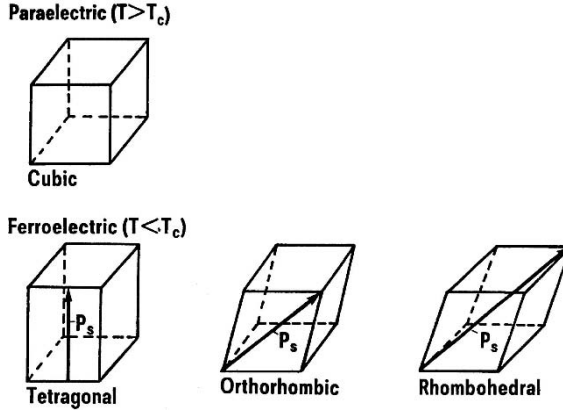


Fig. 3.4. The four phases of BaTiO₃. The arrows indicate the direction of the spontaneous polarization related to spontaneous cell deformation

At every transition the Ti ion adopts its privileged partnership with O ions or, in terms of chemistry or covalent bonds, its coordination number. In the cubic phase it moves statistically among all its six oxygen neighbors, in the tetragonal phase among five neighbors, in the orthorhombic phase among four neighbors, and in the rhombohedral phase, finally, it is coordinated to three oxygen ions. Owing to the lattice distortion, these coordinations can be exactly equivalent only in the cubic and in the rhombohedral case, and it should be emphasized once more that they describe the homopolar picture only and do not include the heteropolar part of the binding. The described phase transitions are summarized and visualized once more in Fig. 3.4.

In order to make the further discussions of this chapter as simple as possible, it is important that all features discussed up to now are explained also quantitatively by the phenomenological Landau–Ginsburg–Devonshire thermodynamic theory [4], which is based on relatively simple assumptions. Devonshire used the cubic state as the basic or prototype phase and treated the ferroelectric distortions as minor deviations. For this reason, he has expanded the free energy A around the cubic state ($A = A_0$) in ascending power of the polarization, which he used as measure for the distortions. Because of the symmetry of the cubic perovskite lattice, there are no terms exhibiting odd powers of $P_{1,2,3}$ and one gets an expression

$$A = A_0 + \frac{\chi}{2} (P_1^2 + P_2^2 + P_3^2) + \frac{1}{4} \xi_{11} (P_1^4 + P_2^4 + P_3^4) + \text{terms of higher order.} \quad (3.4)$$

Because of the general relation

$$\partial A / \partial \vec{P} = \vec{E}, \quad (3.5)$$

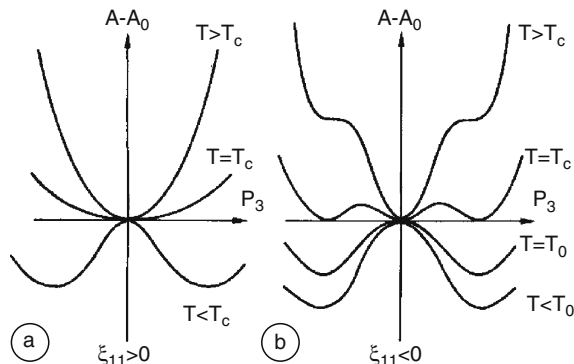


Fig. 3.5. Free energy of BaTiO₃ as plotted vs lattice polarization P_3 (schematically)

one gets in the case of high permittivity ($\epsilon \gg \epsilon_0$ or $\mathbf{D} \approx \mathbf{P}$) from the Curie–Weiss law (Eq. 3.1) as valid in the cubic state

$$\chi \cong \frac{T - T_0}{\epsilon_0 C}. \quad (3.6)$$

Now, in the Devonshire theory the validity of (3.4) is extended to the region below the Curie temperature. Furthermore, it is assumed that all terms of higher power in (3.4) do not depend on temperature significantly. Under these assumptions, (3.4) represents a family of curves as shown in Fig. 3.5, where $A - A_0$ is plotted versus the polarization for different temperatures. It should be noted that the Devonshire equation needs only the correct adaptation of three constants for a roughly correct description of the permittivity, polarization, and phase transitions observed in BT. In this description, the observed lattice distortions are nothing but the electrostrictive consequence of the spontaneous polarization (cf. Fig. 3.4).

Let us go back to Fig. 3.5, which describes the neighborhood of the Curie temperature. In the case of Fig. 3.5a, no secondary minimum exists above the Curie temperature and the curve of free energy is nearly parabolic with a curvature corresponding to the Curie–Weiss law. Below T_C , the central minimum becomes unstable and lateral minima develop in the (100) directions. This represents a thermodynamic transition to a ferroelectric state of second order. On the contrary, in case the side minima pre-exist above the Curie temperature, owing to the already mentioned influence of covalency, the diagram of $(A - A_0)$ vs. \mathbf{P} transforms to the shape in Fig. 3.5b. The central minimum and the (100) minima coexist within a limited temperature region, whether they are stable or metastable. The transition from the non-ferroelectric cubic state to the tetragonal ferroelectric state is of first order.

As mentioned already, on cooling down further two more ferroelectric phase transitions occur. Both are of first order as shown in the complete

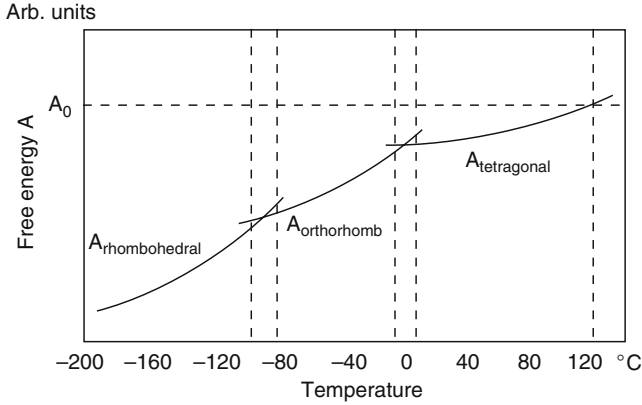


Fig. 3.6. The free energy of the different ferroelectric phases of BaTiO_3 as a function of temperature (schematic)

energy phase diagram of BT (Fig. 3.6), where we have plotted the free energy of the possible phases vs. temperature. Of course, the stable phase is represented by the lowest curve. But owing to the fact that we are dealing with very small energy differences, especially near the transitions themselves, the apparent properties often are co-determined by the neighboring metastable phases.

Generalizing, we may call a phase ferroelectric when it has two or more polar states (in the absence of an electric field) that can be shifted or switched from one to another by an electric field. The polar character of these orientation states must represent a completely stable configuration in zero field. Ferroelectrics are therefore often considered to belong to the subgroup of the 10 polar crystal classes⁴ that are capable of being switched in some manner. The possibility of switching usually implies a polar structure characterized by small distortions from a higher-symmetry non-ferroelectric phase, which is termed the *prototype phase*. Although the prototype phase is not necessarily of nonpolar character, it proves to be so for the vast majority of known ferroelectrics, and in the following we shall make this assumption generally.

As a result of the small structural displacements from the prototype phase, a typical ferroelectric possesses a spontaneous polarization P_s , which decreases with increasing temperature T , to disappear continuously, or more often discontinuously, at a certain temperature, the so-called Curie temperature T_c . The phase above the Curie point is usually termed *paraelectric*. It is not, of course, necessary that the paraelectric phase be the prototype phase, although this is quite often the case.

A ferroelectric transition is usually connected with the condensation of a soft polar or optically active mode of lattice motion at the Brillouin-zone

⁴ These classes are called polar because they possess a spontaneous polarization or electric moment per unit volume.